Check for updates

Received: 4 April 2023 Revised: 21 June 2023 Accepted: 10 July 2023

DOI: 10.1002/rpm.20230003

REVIEW ARTICLE

RESPONSIVE MATERIALS Open Access WILEY

Functional heterophasic liquid metals

Yan Peng[1] | Yumeng Xin[2] | Jiuyang Zhang[1] | Michael D. Dickey[3] | Quan Li[1]

[1]Institute of Advanced Materials and School of Chemistry and Chemical Engineering, Southeast University, Nanjing, China

[2]Jiangsu Key Laboratory of Function Control Technology for Advanced Materials, School of Environmental and Chemical Engineering, Jiangsu Ocean University, Lianyungang, China

[3]Department of Chemical and Biomolecular Engineering, North Carolina State University, Raleigh, North Carolina, USA

Correspondence

Jiuyang Zhang, Michael D. Dickey, and Quan Li.
Email: jiuyang@seu.edu.cn, mddickey@ncsu.edu, and quanli3273@gmail.com

Abstract

Liquid metals (LMs) have compelling applications in stretchable electronics, wearable devices, and soft robotics ascribing to the unique combination of room temperature fluidity and metallic electrical/thermal conductivity. Adding metallic elements in gallium-based LMs can produce heterophasic (i.e., solid and liquid) LMs with altered properties including morphology, surface energy, rheology, electrical/thermal conductivity, and chemical reactivity. Importantly, heterophasic LMs can respond to external stimuli such as magnetic fields, temperature, and force. Thus, heterophasic LMs can broaden the potential applications of LMs. This report reviews the recent progress about heterophasic LMs through metallic elements in the periodic table and discusses their functionalities. The heterophasic LMs are systematically organized into four categories based on their features and applications including electrical/thermal conductivity, magnetic property, catalysis/ energy management, and biomedical applications. This comprehensive review is aimed to help summarize the field and identify new opportunities for future studies.

Keywords

electronics, functionality, gallium, heterophasic, liquid metal

1 | INTRODUCTION

Metals are an important category of materials owing to their superior mechanical properties, high density, and excellent electrical/thermal conductivities.[1–4] Over one thousand years of blacksmith's technology have made metals into desired shapes, yet such approaches require high energy consumption. The high moduli of most metals lead to processing challenges as well as the significant incompatibility with emerging types of soft electronics. Liquid metal (LM) —that is, metals with low melting points near room temperature—addresses these issues and have received increased attention in various fields.[5–8]

Ga-based LMs are fascinating materials due to the intriguing combination of room-temperature fluidity, low viscosity, and negligible toxicity combined with metallic thermal/electrical conductivity.[9–11] Such interesting combination of properties makes Ga-based LMs suitable for care.[16] Nevertheless, broadening the applications of LM is restricted by the following:

applications in stretchable electronics,[12] thermal management,[13] chemical catalysis,[14,15] and biomedical health

(1) Commercial LMs consist of gallium and its alloys such as eutectic Ga-In (EGaIn) and Ga-In-Sn (Galinstan). While these metals have interesting properties, they are limited. For example, they are diamagnetic and thus, not responsive to magnetic fields.
(2) Commercial LMs have fixed melting points and phase behavior.[17] The ability to change the phase behavior would broaden the application space.

This is an open access article under the terms of the Creative Commons Attribution License, which permits use, distribution and reproduction in any medium, provided

(3) Most LM-polymer composites consist of LM dispersed in polymer and therefore are typically insulating. While these LM-polymer composites can be rendered conductive with sophisticated designs or treatments, simpler methods are preferable.[18,19]
(4) LMs have low viscosity. The leakage phenomenon is a common issue during the operation of LMs due to its constant low viscosity. The ability to vary the rheology would make it easier to print it from a nozzle and also make it less likely to leak from devices.

To address the above issues, research has been combining Ga-based LM with other metallic elements to tune the functionality.[20–25] The solid metals in the LMs (that forms heterophasic LMs in this review) not only address the above challenges but also bring new features into the heterophasic LMs.[26–28] We list several examples:

(1) Adding metal elements to LMs can endow the resulting heterophasic LMs with distinctive functionality such as magnetic responsiveness from LM-Fe/Gd/Ni,[29–31] superior catalytic activity from LM-Pt/Pd/Rh,[32–34] and biomedical function from LM-Cu/Zn/Mg,[35,36] (Figure 1a, colors represent the functionalities).[43,44]
(2) The properties of heterophasic LMs (e.g., morphology, strength, rheology, electrical/thermal conductivity, and chemical reactivity) can be tuned through compositions and are highly dynamic[38,45] in response to stimuli such as magnetic field and temperature.[46]
(3) While LM-polymer composites are typically insulating, heterophasic LM polymer composited can be electrically conductive.[47–49]
(4) Heterophases in LMs can lower surface tension energy compared with pure LMs.[50] It can also improve wettability and limit leakage of LM from devices.[51,52]

In recent years, due to the excellent features realized by adding elements, a variety of heterophasic LMs have been introduced into different fields such as soft electronics, magnetic robots, catalysis, energy management, and biomedical applications.[43,53–56] This review intends to classify the recent research about heterophasic LMs through a fresh and practical perspective of elements and functionalities (Figure 1). According to the functionalities derived from different metallic elements, heterophasic LMs are systematically organized into four categories in the review as shown in Figure 1b and Table 1. A comprehensive review of the relevant literature is provided to summarize current studies and intends to present a general picture for future studies of LMs.

This article systematically reviews the properties as well as functionalities of heterophasic LMs with different metallic elements. The recent progress in the fields of electrical/thermal conductivity, magnetism, catalysis, energy management, and biomedical application are discussed thoroughly. The heterophasic LMs can overcome the deficiency of LM, improve its performance and introduce new functionalities. The detailed performance and applications of different heterophasic LMs are summarized by figures and tables in each section. The future research directions of heterophasic LMs and the main challenges are proposed, which can inspire innovations for future investigation on heterophasic LMs.

2 | ELECTRICAL AND THERMAL CONDUCTIVITY OF HETEROPHASIC LMs

2.1 | Preparation of heterophasic LMs

Heterophasic LMs can be formed through various established strategies including heating, mechanical blending, acidfacilitated mixing, and electrochemical approach (Table 1).

As demonstrated in the phase diagram, a variety of metals including In, Sn, Bi, Zn, and Ag are soluble in liquid Ga through simply heating and stirring, which produces heterophasic LMs. In addition, the morphological, rheological, thermal, and catalytic properties are highly tunable based on the metallic phase diagram to adapt to different applications. Interestingly, the metallic crystals can be extracted from the LM solvent through reducing the surface tension by applying voltage and vacuum filtration.[57,58] The structure of the crystals exhibits versatile morphological and compositional diversity, which proposes a general approach to construct crystals with controllable and delicate structures for further application.

However, a large proportion of other metals such as Cu and Fe have difficulty dissolving in liquid Ga. Fortunately, the heterophasic LMs can be obtained by mechanical stirring of LM and immiscible metallic particles in an ambient environment. Mechanical stirring increases the contact area of the metals by splitting the particles and disrupting the interfacial oxides. For example, heterophasic LM consist of LM and tungsten (W) can be formed by physical grinding and the obtained LM-W mixture inherits the high thermal conductivity of tungsten.[59] Besides, the immiscible particles can also be "swallowed" by the LM through removing the metal oxide in an acidic environment. For instance, magnetic LMs can be fabricated by mixing iron particles and LM in hydrochloric acid (HCl) solution.[60] The key issue in dispersing immiscible metals in LM is to eliminate the metal oxide that impedes the solid metal particles from entering the LM.

Apart from physical blending, chemical reaction such as galvanic replacement contributes to the formation of the heterophasic LMs. Galvanic replacement reaction (GRR) is an electrochemical process driven by the electrochemical potentials difference of two metals. During this process, the metal with higher potential is reduced and deposits at the cathode. The simple GRR has been widely used for the generation of controllable metallic nanostructures. For instance, the metallic core-shell structure can be obtained through the galvanic replacement between $KAuBr_4$ and LMs.[61]

28348966, 2023, 1, Downloaded from https://onlinelibrary.wiley.com/doi/10.1002/rpm.20230003, Wiley Online Library on [22/03/2024]. See the Terms and Conditions (https://onlinelibrary.wiley.com/terms-and-conditions) on Wiley Online Library for rules of use; OA articles are governed by the applicable Creative Commons License

2.2 | Electrical conductivity of heterophasic LMs

Ga-based LM with excellent fluidity, negligible toxicity, and high electrical as well as thermal conductivity is receiving increasing attention in metal–polymer composites.[62–64] However, in most cases, the composites are not inherently conductive because they are not in intimate contact. The LM particles (LMPs) have to be sintered (e.g., mechanical, hightemperature, and laser sintering) to rupture the native oxide of LM to form a continuous percolating network in the polymeric matrix.[65] Fortunately, adding solid metal particles into liquid gallium that are biphasic or heterophasic LMs will avoid the sintering procedure and directly form uniform electrically conductive route in polymers (Table 1).[66–68] This is because the rigid solid phase in heterophasic LM could penetrate the coverage of polymer and connect the LM to form conductive networks in polymer matrix (Figure 2f).

To realize electrically conductive LM composites, researchers have added solid metal particles (Cu, Ag, Ni, and W) into LM. The resulting composites are conductive, stretchable, and thus useful for stretchable electronics.[71–73]

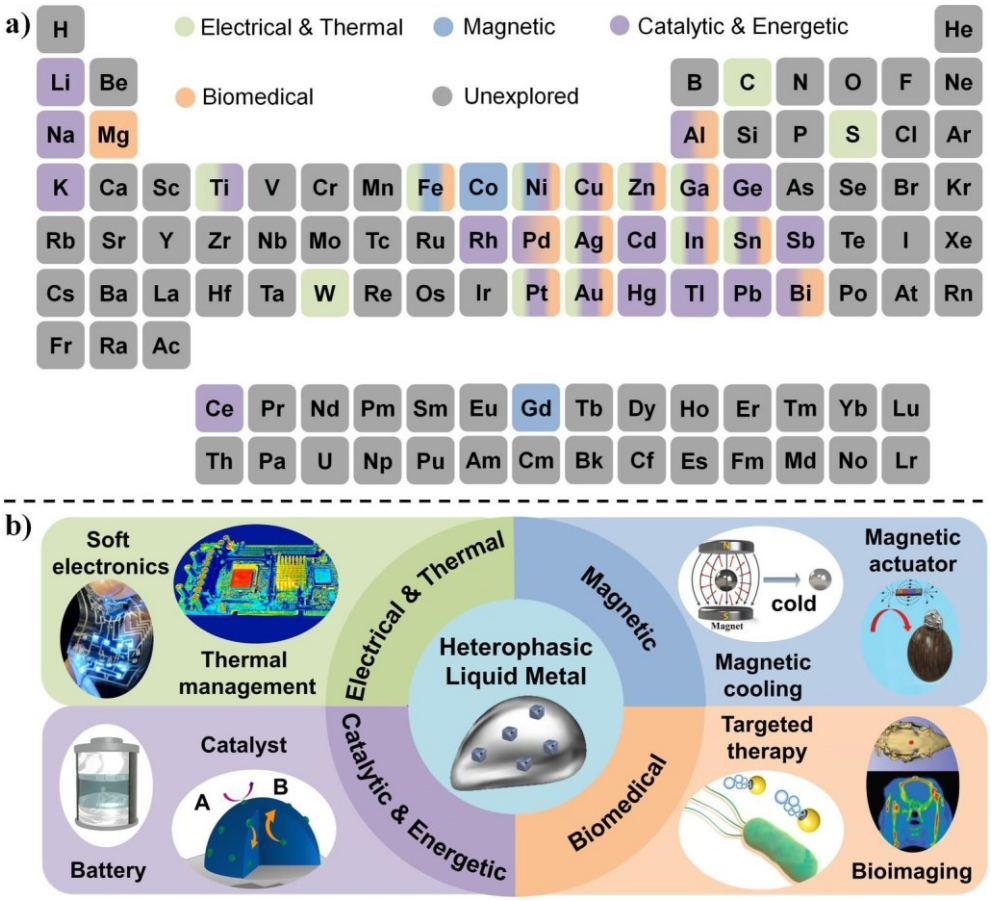

FIGURE 1 (a) Adding elements to Ga-based LMs can create heterophasic LMs that exhibit varied functionalities, including electrical and thermal, magnetic, catalytic and energetic, and biomedical functions. Different colors represent different functionalities. The elements with multifunctionalities are represented with a gradient color. For example, heterophasic LM with iron (Fe) element exhibits enhanced electrical conductivity, magnetic response and biomedical utility. For the preparation of the heterophasic LMs, it should be noted that the mixing of metallic elements in liquid metals is usually limited by the surface oxides of LM (although the native oxide contributes to the adhesion of LM on substrate). There are several approaches for the synthesis of heterophasic LMs to overcome the challenges. Increasing the temperature, grinding, and applying mechanical stirring or sonication would accelerate the mixing of the solid metals and LMs. In addition, the oxide layer can be removed via chemical dissolution with acids or bases such as HCl or NaOH. In addition, electrochemical strategy is also a promising method to dissolve various metals into LMs. (b) Appealing features and corresponding applications of different heterophasic LMs. Reproduced with permission.[37] Copyright 2021, Springer Nature. Reproduced with permission.[38] Copyright 2022, National Academy of Sciences. Reproduced with permission.[39] Copyright 2021, American Chemical Society. Reproduced with permission.[40] Copyright 2021, Wiley-VCH. Reproduced with permission.[33] Copyright 2021, American Chemical Society. Reproduced with permission.[41] Copyright 2020, Wiley-VCH. Reproduced with permission.[36] Copyright 2021, Wiley-VCH. Reproduced with permission.[42] Copyright 2020, the Royal Society of Chemistry. LMs, liquid metals.

For example, the electrical limitation can be eliminated by coating highly conductive metals on the surface of LM micro or nanoparticles (GRR).[61] As shown in Figure 2a, the metallic core-shell structure is available through the galvanic replacement between alkaline $KAuBr_4$ and LMs with the aid of surfactants. By sonication and galvanic reaction, Au/$AuGa_2$ encapsulated stable sub-micrometer Ga-alloy droplets are successfully synthesized and applied by drop casting a film. Core-shell structural Ag@LM particles are also obtained by in situ coating nano-silver on the surface of LMPs.[74] Due to the features of sintering-free initial conductivity (8.0 Ω sq^{-1}), real-time self-repairing, and electrical durability, the Ag@LMP are a promising candidate to fabricate self-healing flexible circuit (such as NFC tags,

28348966, 2023, 1, Downloaded from https://onlinelibrary.wiley.com/doi/10.1002/rpm.20230003, Wiley Online Library on [22/03/2024]. See the Terms and Conditions (https://onlinelibrary.wiley.com/terms-and-conditions) on Wiley Online Library for rules of use; OA articles are governed by the applicable Creative Commons License

TABLE 1 Detailed information of heterophasic LMs with enhanced properties.

Function	Composition	Features	Preparation	Application	Ref.
Electrical property	Au-Ga	4.3 Ω	Chemical reaction	Drop casting noble metal-LM circuits	[61]
	AgNWs-LM	8.65 10^5 Sm^{-1}	Laser-irradiating	Complex stretchable circuitry	[73]
	Fe-, Au-LM	1.1 Ω·m/0.5 Ω sq^{-1}	Stirring/deposition	Multilayer circuits, sensors, and actuators	[67, 70]
	Ga-In	Tunable: 1–10^8 Ω	Heating	Flexible thermal conductors and sensors	[45]
Thermal property	Cu-LM	50 W m_{-1} K_{-1}	Stirring in solution under 5 V	Thermal interface materials	[79]
	Cu-LM	65.9 W m_{-1} K_{-1}	Chemical modification	Electronics thermal management	[77]
	W-Ga	57 W m_{-1} K_{-1}	Grinding		[59]
	Ga-In-Sn	20.3 W m_{-1} K_{-1}	Heating and stirring		[38]
Magnetic property	Fe-LM	Tunable mechanical properties, viscosity, and stiffness	Stirring in HCl	Wearable electronics, implantable devices and magnetic manipulation	[40, 60]
	NdFeB-LM	Reversible transition and morphological adaptability	Mechanical mixing	Flexible erasable recording paper and controllable miniature robotics	[85, 86]
	Gd-LM	Magnetocaloric effect	Grinding	Magnetically controlled cooling	[39]
	Fe-LM	Self-healing, locomotion and shape deformation	Submerging in HCl under magnetic field	Magnetically controlled locomotion	[87]
Catalytic property	Ga-Ag	92% efficiency	Sonication and stirring	CO_2 conversion	[95]
	Pt-, Rh- and Pd-Ga	Productivity: 80–263 $g_{propene}g_{Pt-1}$	Sonication	Akanes dehydrogenation	[33, 34, 91, 96]
	Pt-Ga	Activity: 2.8 10^7 mA mg_{Pt}^{-1}	400°C heating	Oxidation, reduction and electrochemical reactions	[32]
Energetic property	Na/Li^+-Ga/In	Discharge capacity for Li: 706 mAh g^{-1} Na 222.3 mAh g^{-1}	Heating, sonication and stirring	Energy storage devices	[101]
	Ga-Sn	Faradaic efficiency: >95%	Shaking	High-specific-energy batteries	[102]
	Na-K-Ga	Capacity retention: 99.95% Coulombic efficiency: 100%	Mixing	Energy storage devices	[41]
Biomedical property	Cu-LM	Radiographic capabilities	Mixing in NaOH	CT assistant localization	[42]
	Cu-LM	Pathogens eradication: 99%	Chemical reactions	Antimicrobial and antiviral fabrics	[107]
	Fe-, Zn-LM	High antibacterial efficiency	Coating/Doping	Bacterial treatment	[36, 109]
	Pd-LM	Photothermal effect and photoenhanced catalysis	Sonication in PVP solution	Tumor inhibition	[110]

flexible cables, and direct writing circuit). Another unique Pt-LM Janus structure in Figure 2b is constructed by sputtering Pt onto one hemisphere of an LM microsphere. These chemically powered biphasic metallic particles can target and weld silver nanowires (AgNWs) to improve the electrical conductivity of the AgNW network.[69] Moreover, a laser-irradiated metallic composite (LIBMC) with biphasic metallic fillers (LM and AgNW) is reported to have programmable electrical properties and outstanding stretchability.[73] Although the high fluidity of LM makes it suitable for stretchable electronics, the deformation-induced resistive change of LM composite limits the applications of LM in conductors. On the contrary, the LIBMC conductor exhibits robust electrical and mechanical features by creating contact between discrete LMPs and AgNW network. The existence of biphasic metal enables direct, uniform, and durable patterning of conductive layer on the stretchable substrate.

It is convenient to introduce solid metals into LMs via mechanical agitation or other physical means to create heterophasic systems.[75,76] Biphasic LM composites consisting of LM and solid metal fillers[66] (Ag flakes, Ag-coated-Ni, Ag-coated-Fe, Ni, etc.) can form conductive ternary material systems by combining them with block

28348966, 2023, 1, Downloaded from https://onlinelibrary.wiley.com/doi/10.1002/rpm.20230003, Wiley Online Library on [22/03/2024]. See the Terms and Conditions (https://onlinelibrary.wiley.com/terms-and-conditions) on Wiley Online Library for rules of use; OA articles are governed by the applicable Creative Commons License

copolymer binder. The resulting composites are intrinsically conductive without any sintering. Such heterogeneous materials can also form super elastic, healable, and durable conductors by mixing conductive fillers (Ag flakes) with eutectic gallium indium particles and thermoplastic elastomers.[51] Moreover, the composites can form sinter-free conductive inks that can be used to deposit thin, highly conductive, and mechanically robust semiliquid circuit traces on a wide range of substrates.[50] The enhanced properties of conductive ink are achieved through the bonding of Ag nanoparticles by LM and the circuit can even be printed on 3D surface with complex shapes.

As shown in Figure 2c, Au is widely combined with LM to achieve high conductivity and outstanding stretchability. For example, it can be used as a substrate to deposit LM to form biphasic solid–liquid thin metal films.[70] Due to the high surface tension of an LM, it tends to form isolated particles during thermal evaporation onto surfaces. This issue can be addressed by depositing it onto a thin layer of gold, to which it reactively wets to form $AuGa_2$ (s). The asprepared thin film with liquid Ga and solid $AuGa_2$ shows excellent electrical and mechanical performance, pattern ability as well as scalability.

Iron powders have been incorporated into LM to form LM-filled magnetorheological elastomer (Figure 2d) with anisotropic and unconventional piezoconductivity (i.e., conductivity that changes with deformation of the composite).[67] Interestingly, the mechanical, magnetic, and thermal properties of these heterophasic materials also exhibit significant anisotropy due to the directional alignment of the Fe microparticles under magnetic fields in the matrix. In addition, the electrical conductivity of the composite increases thousands of times in response to small strain, which is attributed to the connection of LM microdroplets between ferromagnetic microparticles. Such strain-sensitive

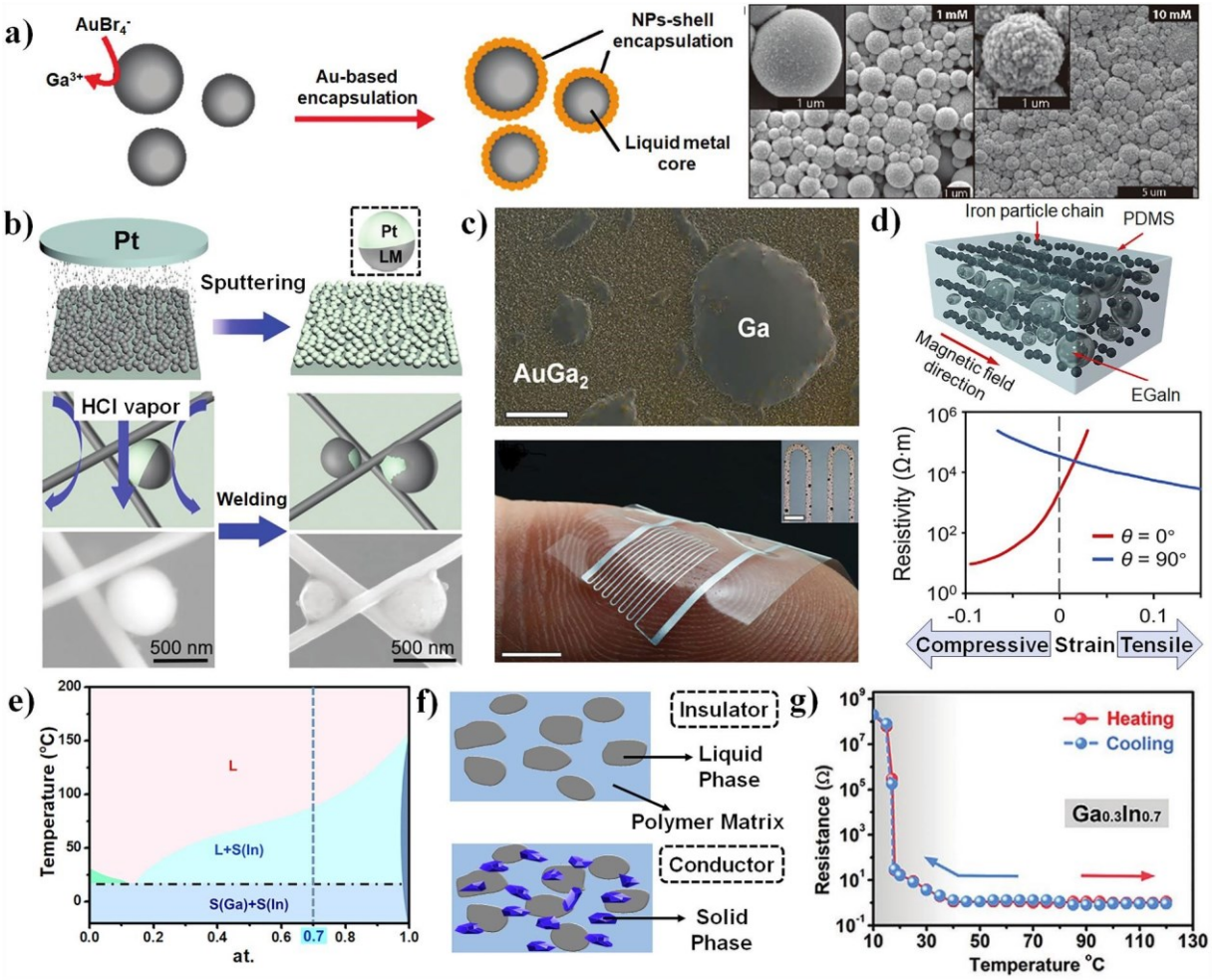

FIGURE 2 Enhanced electrical conductivity of heterophasic liquid materials. (a) Left: Galvanic replacement reaction on the LM droplets and the formation of Au encapsulated structures. Right: SEM images of deposited $AuGa_2$-LM and Au-LM after galvanic replacement; Reproduced with permission.[61] Copyright 2019, the Royal Society of Chemistry. (b) Top: Fabrication of the LM–Pt Janus particles through sputtering Pt onto LM monolayers. Bottom: Schematic illustration and SEM images for the microwelding of AgNW by LM–Pt Janus particles under HCl vapor. Reproduced with permission.[69] Copyright 2019, Wiley-VCH. (c) Top: The microstructure for the surface of Ga-$AuGa_2$ thin layer. Bottom: stretchable biphasic conductor formed by physical vapor deposition of gallium onto an alloying metal film. Reproduced with permission.[70] Copyright 2016, Wiley-VCH. (d) The microstructure and anisotropic property of the LM-filled magnetorheological elastomer. Reproduced with permission.[67] Copyright 2020, Elsevier. (e) Gallium–Indium binary phase diagram. (f) Comparison for the internal network of LMPC and HLMPC. The LMPC is insulated as the LM particles are separated by polymer matrix. While the rigid solid phase added in heterophasic LM could penetrate the coverage of polymer and connect the LM to form conductive networks in polymer matrix, leading the HLMPC an intrinsic conductor. (g) The temperature dependent resistive change of binary metal composite. Reproduced with permission.[45] Copyright 2021, Wiley-VCH. HLMPC, heterophasic LM-polymer composites; LM, liquid metal; LMPC, LM-polymer composites.

28348966, 2023, 1, Downloaded from https://onlinelibrary.wiley.com/doi/10.1002/rpm.20230003, Wiley Online Library on [22/03/2024]. See the Terms and Conditions (https://onlinelibrary.wiley.com/terms-and-conditions) on Wiley Online Library for rules of use; OA articles are governed by the applicable Creative Commons License

composites are useful for sensing touch or physical deformation.

As shown in Figure 2e, there are five regions in the Ga-In phase diagram including two solid region (S(In) and S (Ga) + S(In)), two solid–liquid biphasic regions (L + S(In) and L + S(Ga)), and one liquid region (L(Ga + In)). The ratio of solid to liquid in binary metal (BM) materials can be conveniently controlled through composition and temperature regulation based on the classical phase diagram. The principles can be used to form a dynamic stretchable polymer composite with a reversible electrical transition by introducing the BM into polymers.[45] Compared with eutectic LMs, BM has the continuous phase transition and unique temperature dependent properties (fluidity, viscosity, solid fraction, and surface morphology). Specifically, the composition of the liquid and solid phases in BM gradually changes (that is so-called "continuous" transition) as a function of temperature during the phase transition, transferring from solid alloy (S(Ga) + S(In)) to slushes (L + S (In)), and finally monophasic LM (L(Ga + In)). Therefore, the phase transition controlled by temperature regulation leads to the reversible electrical transition of the BM composite between insulator and conductor (Figure 2g). There are microgaps between adjacent BM particles under low temperature. When the temperature increased, the BM gradually melts to fill the original poor contact area, leading to decreased resistance of BM polymer. While cooling, the microgaps regenerate due to the fact that LMs will possibly move to solid seeds to have recrystallization in the system.

2.3 | Thermal properties of heterophasic LMs

The addition of solid metals to LM can enhance the thermal conductivity and change the rheology to minimize leakage of LM during stress loading.[77] Generally, high thermal conductivity is associated with fast heat dissipation, which is of great importance to avoid heat damage in electronics. Therefore, rigid metals such as Cu, Ag, Ni, and W are mixed LM to build heterophasic materials for thermal management.[22] Through mechanical mixing, the native gallium oxide (Ga_2O_3) will break and reform continuously. The oxide helps LM and solid particles mix by creating a thin film that encases the particles.[78]

A series of stable semiliquid gallium-based LM composites are prepared with high electrical (6 10^6 S m^{-1}) and thermal (50 W m^{-1} K^{-1}) conductivity through packing the LM with copper particles[79] (Figure 3a). The contacts of the solids and liquids among the particles in the composite significantly improved the heat transfer and the electrical connection. Such LM-Cu materials can be 3D printed as a paste and ultimately convert to $CuGa_2$ solid alloys, which implies it is possible to print metals at room temperature that convert to solids with high melting points postprinting.[80] The inclusion of solid particles in LM can increase the roughness of the heterophasic LM, which enhances the wettability to most substrates (Figure 3b). In addition, the transitional-state metallic mixtures exhibit appealing properties such as chemical stability, tunable viscosity, and selfhealing ability, endowing potential applications in fields such as printed and flexible electronics and thermal interface materials.

Cu and LMPs can be brought closer together for more intimate heat transfer by using interfacial engineering.[77] As shown in Figure 3c, a silane treatment of Cu serves as effective thermal linkers and diffusion barriers at the Ga oxide-Cu interfaces, further improving the thermal conductivity (65.9 W m^{-1} K^{-1}) and stability of the modified LM-Cu composites.

The stability of composites of LM with other metals can be improved by using metals such as W that do not alloy with Ga. W is interesting because it has a high thermal conductivity of 173 W m^{-1} K^{-1}. Through the formation of chemically stable LM-W mixture, the moderate thermal conductivity of LM can be enhanced and the surfacespreading as well as pump-out issues (describes the tendency for LM-based grease to squeeze out of the interface gap due to thermo–mechanical cycling) can be addressed[59] (Figure 3d).

Heterophasic systems have been introduced into the soft materials for the heat dissipation of stretchable electronics. Such systems can be formed by incorporating a series of solid microparticles (Fe, Cu, Ag, and Ni) into LM and then dispersing this suspension in a soft, highly extensible silicone elastomer.[81] These flexible materials have a thermal conductivity of 11.0 0.5 W m^{-1} K^{-1} when strained. Concepts from classical ternary phase diagram can be used to enhance the thermal management.[38] In addition to metallic thermal conductivity, the ternary metal (TM) possesses wide phase transition temperature range and high effective latent heat (The enthalpy actually used for devices in the working temperature ranges from 30 to 70°C) compared to room temperature LM-based thermal grease. Figure 3e shows the liquidus projection with isotherms of the ternary phase diagram. The Ga-In-Sn ternary phase diagram can be thought as the combination of three binary phase diagrams of Ga-In, Ga-Sn, and In-Sn. The E_0e_1, E_0e_2, and E_0e_3 refer to the eutectic curves of the system, under which the TMs are completely solid. Different from binary metals, TM passes through two solid–liquid biphasic regions and eventually turns into a homogeneous single liquid phase as the temperature increases. The triple-phase transitions upon heating contribute to high effective latent heat and wide service temperature window of TM as the Differential Scanning Calorimetry (DSC) curves shown. More importantly, the melting range, latent heat, and fluidity (viscosity) of TMs can be tuned through the composition and temperature regulation to adapt with different service conditions. The elemental composition of TM system can be extended to metals such as Fe and Al to meet the needs of higher working temperature in industrial production.

28348966, 2023, 1, Downloaded from https://onlinelibrary.wiley.com/doi/10.1002/rpm.20230003, Wiley Online Library on [22/03/2024]. See the Terms and Conditions (https://onlinelibrary.wiley.com/terms-and-conditions) on Wiley Online Library for rules of use; OA articles are governed by the applicable Creative Commons License

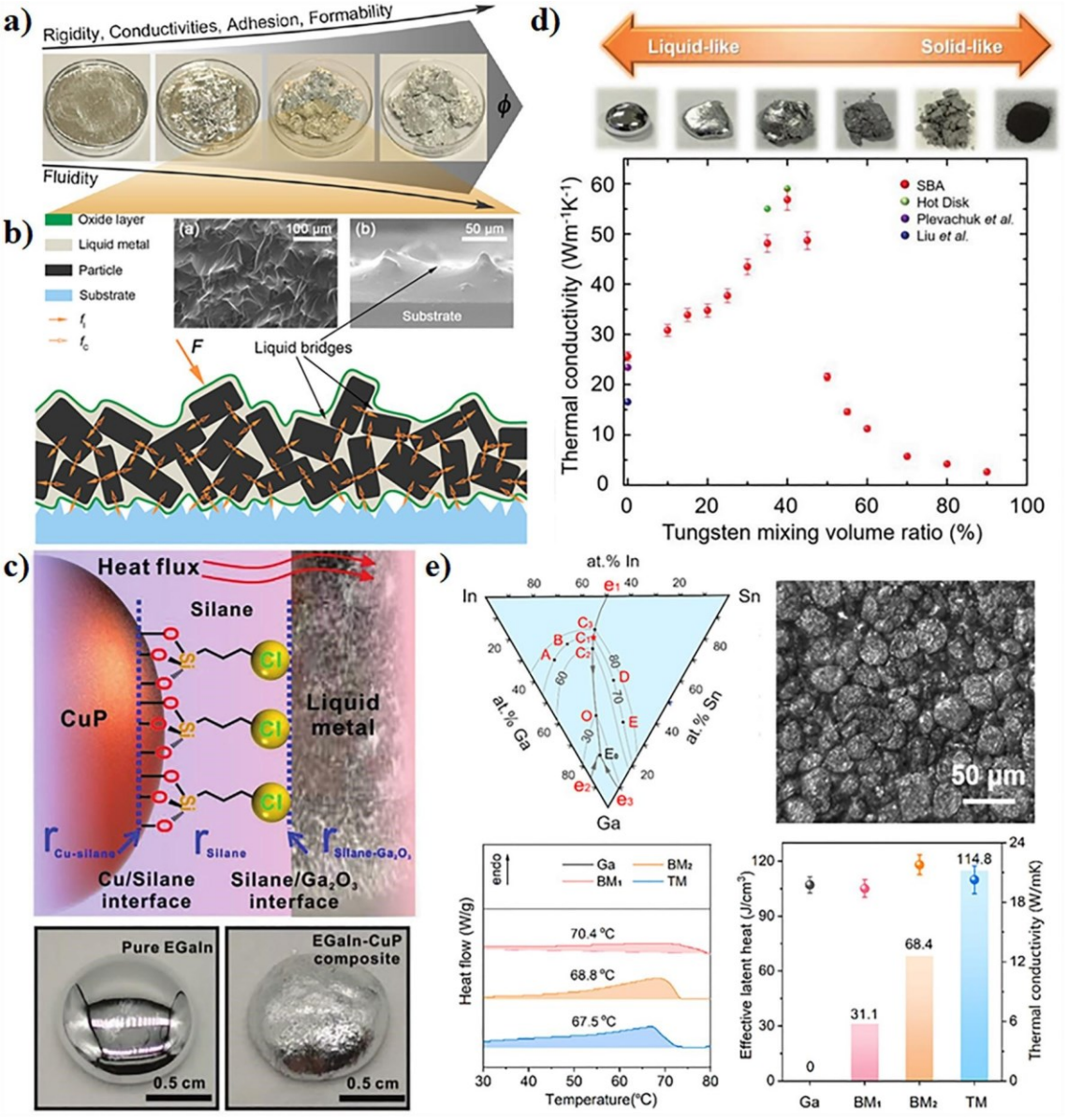

FIGURE 3 Enhanced thermal conductivity of heterophasic liquid materials. (a) Optical photos of transitional-state metallic mixtures. As the content of Cu increased, the composite changed from a liquid-like state to a solid-like state. (b) Schematic illustration for the interaction between the substrate and the heterophasic LM. The solid particles and liquid bridge significantly improved the heat transfer. The surface oxide layer and the internal solid particles both increased the roughness and adhesion of the heterophasic LM. Reproduced with permission.[79] Copyright 2017, American Chemical Society. (c) Top: Schematic illustration of heat conduction between the interface of CuPs and Ga_2O_3. Bottom: Optical images of pure EGaIn and EGaIn composites with modified CuPs. Reproduced with permission.[77] Copyright 2021, Wiley-VCH. (d) The optical photo and thermal conductivity of LM-W mixtures contained different volume ratios of W microparticle inclusions as measured using the step-bar apparatus (SBA, a method to measure thermal conductivity). Images of LM-W beginning as a LM and transitioning from a liquid-like to a solid-like material as more tungsten particles are added, eventually becoming granular-like pure tungsten powder. Reproduced with permission.[59] Copyright 2019, Wiley-VCH. (e) Top: Ga-In-Sn ternary phase diagram and optical photos for the thermal grease with ternary metal. Bottom: The ternary metal exhibits high enthalpy of fusion (latent heat, calculated from the integration of the shadowed areas) and thermal conductivity (dots) compared with LM and binary metal. Reproduced with permission.[38] Copyright 2022, National Academy of Sciences. CuPs, Cu particles; LM, liquid metal.

3 | MAGNETIC HETEROPHASIC LMs

As a noninvasive and highly selective stimulus, magnetic fields can realize remote and penetrating control of magnetoactive materials without influencing the nonmagnetic materials.[82–84] For example, it can penetrate into tissue. It is well known that gallium is a diamagnetic material, which means it does not move in response to magnetic fields. Fortunately, magnetic materials can be added to LM. Fe, Co, and Ni particles combined with LM endow the LM with magnetic responsiveness, which has applications for moving metal for electronic cooling, robotic actuation, and microfluidic patterning (Table 1). For instance, Fe particles can disperse in LM using a dilute hydrogen chloride (HCl) solution to remove surface oxide.[60] The viscosity and stiffness of LMFe composites can be increased by adding more Fe. More importantly, the inner magnetic Fe particles align along the magnetic field lines, as shown in Figure 4a. Consequently, the mechanical properties of the LM-Fe slurry could be reversibly tuned by an external magnetic field. Due to the high conductivity, reversibly tunable stiffness, and excellent biocompatibility, the LM-Fe composites show great potential in both wearable electronics and implantable devices. Interestingly, the LM-based

28348966, 2023, 1, Downloaded from https://onlinelibrary.wiley.com/doi/10.1002/rpm.20230003, Wiley Online Library on [22/03/2024]. See the Terms and Conditions (https://onlinelibrary.wiley.com/terms-and-conditions) on Wiley Online Library for rules of use; OA articles are governed by the applicable Creative Commons License

ferrofluid possesses convenient phase transition between liquid and solid states. Through melting and solidification of the LM matrix, the transitional ferrofluid exhibited switchable adhesion and interlocking forces (Interlocking means two objects fitting perfectly so that they connect and move together. Rough surfaces with matchable irregularities get interlocked when contact with each other due to the friction force) to grasp nonmagnetic objects[40] (Figure 4b). A magnetic field could be applied to manipulate and transport the objects, which release on demand by using electromagnetic induction heating to melt the metal. Thus, the whole magnetic manipulation of arbitrarily shaped objects was realized without any other treatments to the target objects. Besides, a magnetoactive phase transitional material (MPTM) is built through dispersing magnetic microparticles in LM.[86] Similarly, the MPTMs can also realize reversible transition between solid and liquid state through heating by alternating magnetic field and cooling under ambient temperature. The MPTMs exhibit excellent morphological adaptability such as splitting, merging, and stretching in the liquid phase, which have promising applications in the fields of healthcare, flexible electronics, and controllable robotics.

Composites containing heterophasic LM can be utilized as an ink to realize magnetic-assisted direct writing of stretchable electronics. NdFeB microparticles in LM

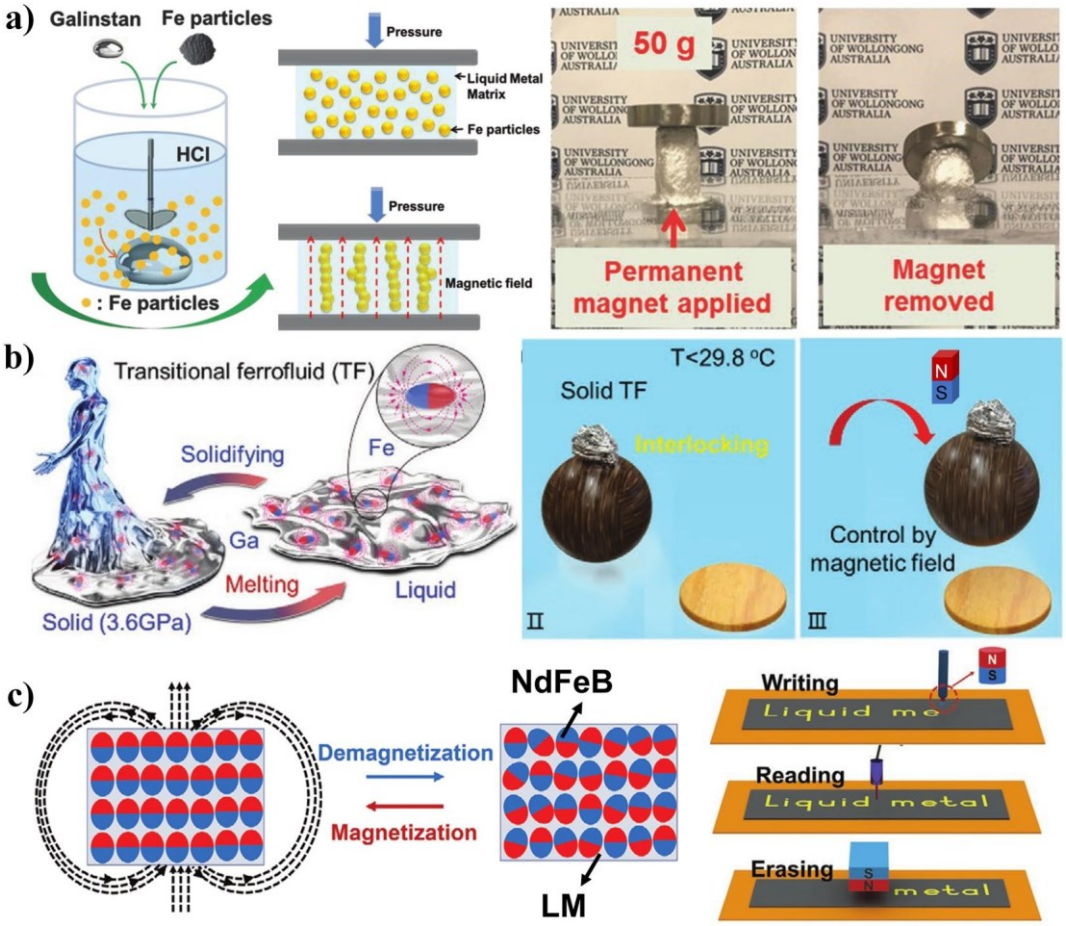

FIGURE 4 Magnetic performance of heterophasic liquid materials. (a) Left: Schematic illustration for the preparation of LM-Fe slurry. The liquid Galinstan becomes slurry-like after mixing with the Fe particles in the HCl solution. Right: Schematic illustration and photos for the LM-Fe slurry with and without magnetic field applied. Chains of Fe particles are formed under the alignment force of magnetic field. Thus, the stiffness of the LM-Fe slurry could be enhanced by applying an external magnetic field. The cylinder under a permanent magnet shows no deformation with a weight on the top. However, the high cylinder topples over immediately after the magnet is removed. Reproduced with permission.[60] Copyright 2018, Wiley-VCH. (b) Left: The reversible phase transition of a TF between solid and liquid. Right: Optical photos for the magnetic grasp of nonmagnetic objects by the phase transition of the TF. The TF solidifies at room temperature (25°C) and tightly interlocks the embedded objects. The embedded objects can be controlled remotely and delivered to the designated spot by a magnetic field. Reproduced with permission.[40] Copyright 2021, Wiley-VCH. (c) Left: Schematic illustration for the magnetization and demagnetization of FM-LMP. Right: Scheme for the writing, reading and erasing process of FM-LMP through magnetic regulation. Reproduced with permission.[85] Copyright 2020, Wiley-VCH. FM-LMP, ferromagnetic LM putty-like material; LM, liquid metal; TF, transitional ferrofluid.

produce inks that can be fully magnetized through a strong impulse of a magnetic field[85] (Figure 4c). The liquid-like suspension turns into ferromagnetic LM putty-like material (FM-LMP) which can be easily remodeled to various shapes and patterned on various substrate. Moreover, the aligned magnetic microparticles become disordered in the absence of the magnetic field, resulting in the demagnetization of the FM-LMP. The process is reversible and the magnetic microparticles can be rearranged to enable macroscopical magnetization. Therefore, the remote magnetic manipulation of FM-LMP resulted in writing, reading (through reading the surface magnetic flux density by Gaussmeter), and erasing of soft substrates, enabling the application of flexible erasable magnetic recording paper.

The element gadolinium (Gd) and some of its alloys have strong magnetocaloric effect (Cooling or heating of magnetic materials when the external magnetic field changes) near room temperature. To create a magnetocaloric ferrofluid, Gd nanoparticles can be combined with LM.[39] The Gd/LM displays spontaneous magnetization and a large magnetocaloric effect as shown in Figure 5a, enabling magnetically controlled cooling.

Magnetic LM can also create shape-deformable, locomotive, and magnetic-field-induced self-healable materials. The MXene-encapsulated magnetic LM (MX-MLM) contains magnetic particles and MXene flakes to realize the nonwettability (from the flakes), high electrical conductivity (from the LM), and locomotion (from the magnetic particles).[87] The shape deformation and locomotion of MXMLM left no traces on surfaces in response to a magnetic field (Figure 5b). Moreover, the mechanical and electrical properties of damaged MX-MLM could be healed under the influence of magnetic field.

The combinations of LM and magnetic metals also have utility for remotely actuated miniature untethered devices for soft robotics. A LM-elastomer magnetic composite (LMMC) with dual-energy transmission mode[88] can shape-morph and locomote under low-frequency field (<100 Hz). Additionally, the LMMC converts the energy from the magnetic field (radio frequency: 20 kHz–300 GHz) to electricity for powering

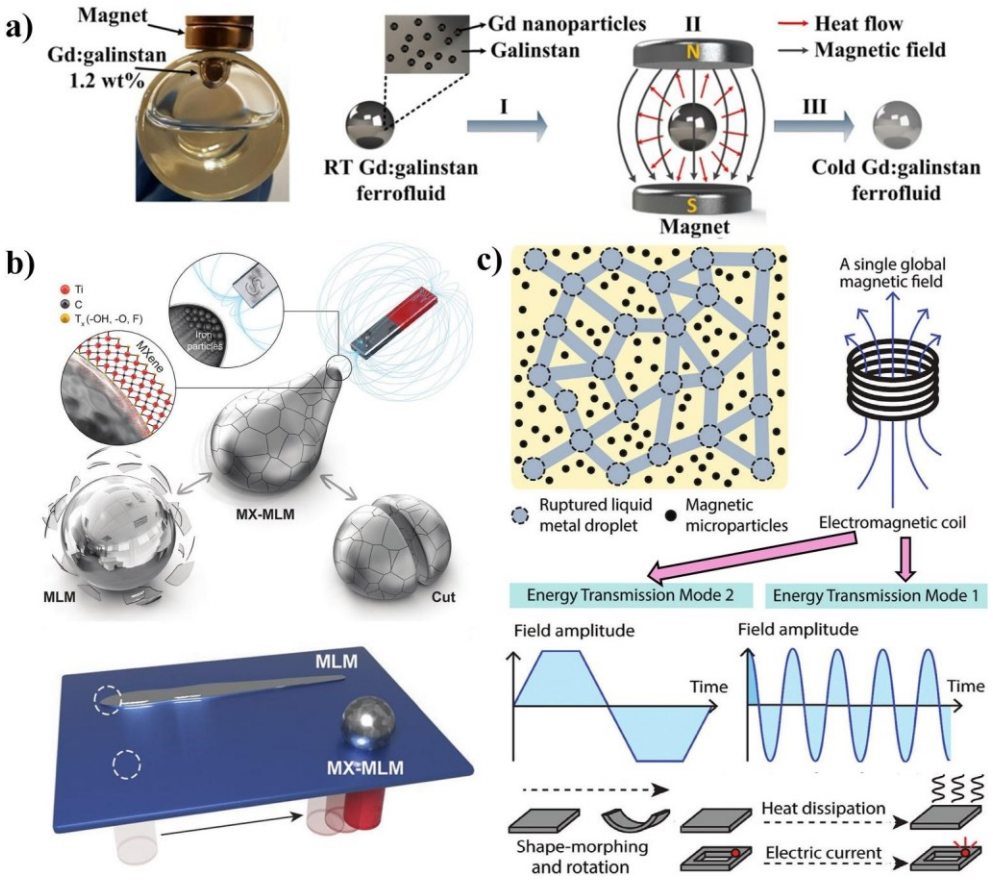

FIGURE 5 Magnetic performance of heterophasic liquid materials. (a) Schematic illustration for the magnetocaloric refrigeration process based on magnetic Gd/LM ferrofluid. The temperature of Gd/LM ferrofluid increases under a magnetic field. The energy is then released to the environment as heat. Finally, the temperature of ferrofluid is lower than that in step I. Reproduced with permission.[39] Copyright 2021, American Chemical Society. (b) Top: Schematic of magnetically induced deformation, recyclability and self-healing of MX–MLM. Bottom: Schematic illustrating translation of MLM using a permanent magnet. Reproduced with permission.[87] Copyright 2022, Wiley-VCH. (c) Scheme for the design and two working principles of the soft composite material. The first energy transmission mode delivers mechanical energy for locomotion under a low-frequency magnetic field. The second energy transmission mode is established by an RF fast-changing component of the magnetic field to deliver heat and electric current. Reproduced with permission.[88] Copyright 2022, Wiley-VCH. MX-MLM, MXene-encapsulated magnetic LM.

28348966, 2023, 1, Downloaded from https://onlinelibrary.wiley.com/doi/10.1002/rpm.20230003, Wiley Online Library on [22/03/2024]. See the Terms and Conditions (https://onlinelibrary.wiley.com/terms-and-conditions) on Wiley Online Library for rules of use; OA articles are governed by the applicable Creative Commons License

electronic device or performing local heating, while maintaining the magnetic-induced manipulation of the materials (Figure 5c). According to the Faraday's law of induction, the induction voltage is produced by the rapid change of the magnetic flux of the robot from the radio-frequency field.

4 | CATALYSIS AND ENERGY APPLICATIONS OF HETEROPHASIC LMs

4.1 | Catalytic performance and efficiency

Catalysis is a key concept for lowering energy requirements to drive reactions.[14] Most traditional solid catalysts have fixed atom arrangement with various inhomogeneous structures, such as different types of crystals, uneven element distribution, abundant lattice defects, and so on. Recently, LM has attracted increasing attention as a catalyst due to its distinct features of rich electrons on the surface, fluidity, negligible vapor pressure, and low toxicity.[89–91] For example, the fluidity allows the metal to be dispersed easily into particles to increase surface area. Likewise, the fluidity of LM can prevent solid products from "coking" the catalyst (that is, sticking to the surface and blocking active sites). The reactivity can be tuned by dissolving or mixing other metals into LM, some of which can migrate to the surface where catalytic reactions occur.

To obtain enhanced catalytic performance and efficiency of different chemical reactions, researchers have developed a lot of heterophasic LMs by integrating LMs with common precious- or transition-metal catalysts (such as cerium [Ce], nickel [Ni], silver [Ag], rhodium [Rh], palladium [Pd], and platinum [Pt], Table 1).[92–94] For example, the reduction of CO_2 is critical for ensuring a future stable climate and developing a sustainable society. CO_2 can be reduced based on Ga-Ag catalyst through mechanical stimuli.[95] The high CO_2 conversion efficiency (92%) and cyclic sustainable process are attributed to the existence of liquid-metal Ga droplets as well as solid silver–gallium rods (Figure 6a). The reaction is attributed to the triboelectric effect of $Ag_{0.72}Ga_{0.28}$ rods under sonication. The localized contact electrification initiates the CO_2 conversion. This work is important because the only energetic input is stirring (mechanical energy).

As another example, Ni, Sn, or Ce addition to LM has some catalytic benefits.[89,93] Converting inert and lowvalued alkanes to reactive and valuable olefins is commercially valuable. Suitable catalysts are critical to obtain high activity and selectivity during the alkane dehydrogenation. Supported catalytically active LM solutions (SCALMS) have proven effective for alkane dehydrogenation[33,34,91] (Figure 6b). When exposed to propane in the form of solidsupported and highly dynamic liquid–solid mixture, Pt-, Rh-, and Pd-Ga systems become very active, selective, and robust alkane dehydrogenation catalysts. Different from traditional solid catalyst, the liquid nature of Ga-based systems not only provides superb catalytic activity, but also effectively prevents deactivation.[96] Besides, the productivity of SCALMS prepared by ultrasonic method is higher than previous reported chemical route indicating a convenient, scalable and efficient heterophasic catalysis.

In addition, heterogeneous catalysts with a solid metal and liquid media can catalyze a variety of reactions. Trace amount of Pt dissolved in liquid Ga could drive a range of catalytic reactions with enhanced kinetics at low temperature[32] (45– 70°C) (Figure 6c). The Ga-Pt heterophasic LM is prepared by dissolving solid Pt beads in liquid Ga at 400°C and then cooled to the desired operating temperature (40–80°C) to evaluate the catalytic activity for different chemical reactions. The catalytic performance of Ga-Pt system is explored by oxidation, reduction, and electrochemical reactions, demonstrating superior catalytic performance than the existing solid platinum catalysts. The high-catalytic activity of the Ga-Pt system is derived from the combined advantages including the activation of Ga atoms, favorable electronic structure and distinct configuration, and the continuous replenishment of mobile Pt atoms at the interface. The importance of the fluidity as well as mobile Pt atoms is evaluated by reduction experiment using solid and liquid Ga–Pt system. Obviously, the solid Ga-Pt system exhibits inferior catalytic activity. Such heterophasic catalyst system with the dynamic interface opens a new window for future exploration of a high-throughput catalysis.

4.2 | Energy harvesting, transformation and storage

In addition, the heterophasic LMs are functional materials for energy harvester, conversion and storage devices (Table 1).[97] Their unique features, such as self-repairing ability, room temperature fusibility, high capacity, and dendrite-free operation, provide new approaches to the challenges in conventional energy materials.[7,98] Among various energy harvesters, the triboelectric nanogenerators (TENGs) could harvest energy from daily motions, which makes TENGs a promising power source for self-powered wearable devices. As exhibited in Figure 7a, LM and silver flakes were embedded in the polymer matrix to build a stretchable and mechanically durable nanogenerator electrode.[99] The system maintained its energy-harvesting performance under extreme deformation as the LM bridged the silver flakes. Moreover, TENGs possess high output voltage, high energy-conversion efficiency, and environmental friendliness, thus significantly expanding the application of deformable energy harvesters.

Converting chemical energy into mechanical propulsion is also explored to produce self-fueled micromotors based on LM composites. A water-driven bubble-propelled micromotor is realized without the aid of energy input.[100] The unique self-propelled micromotor is realized through the asymmetric Janus microstructure coated by Al-Ga binary alloy and Ti. After exposing to water, the ejected hydrogen bubbles provide powerful directional propulsion (Figure 7b), holding considerable promise for applications in industrial

28348966, 2023, 1, Downloaded from https://onlinelibrary.wiley.com/doi/10.1002/rpm.20230003, Wiley Online Library on [22/03/2024]. See the Terms and Conditions (https://onlinelibrary.wiley.com/terms-and-conditions) on Wiley Online Library for rules of use; OA articles are governed by the applicable Creative Commons License

energy conversion devices. Energy storage devices based on LMs are also constructed with high theoretical capacities for

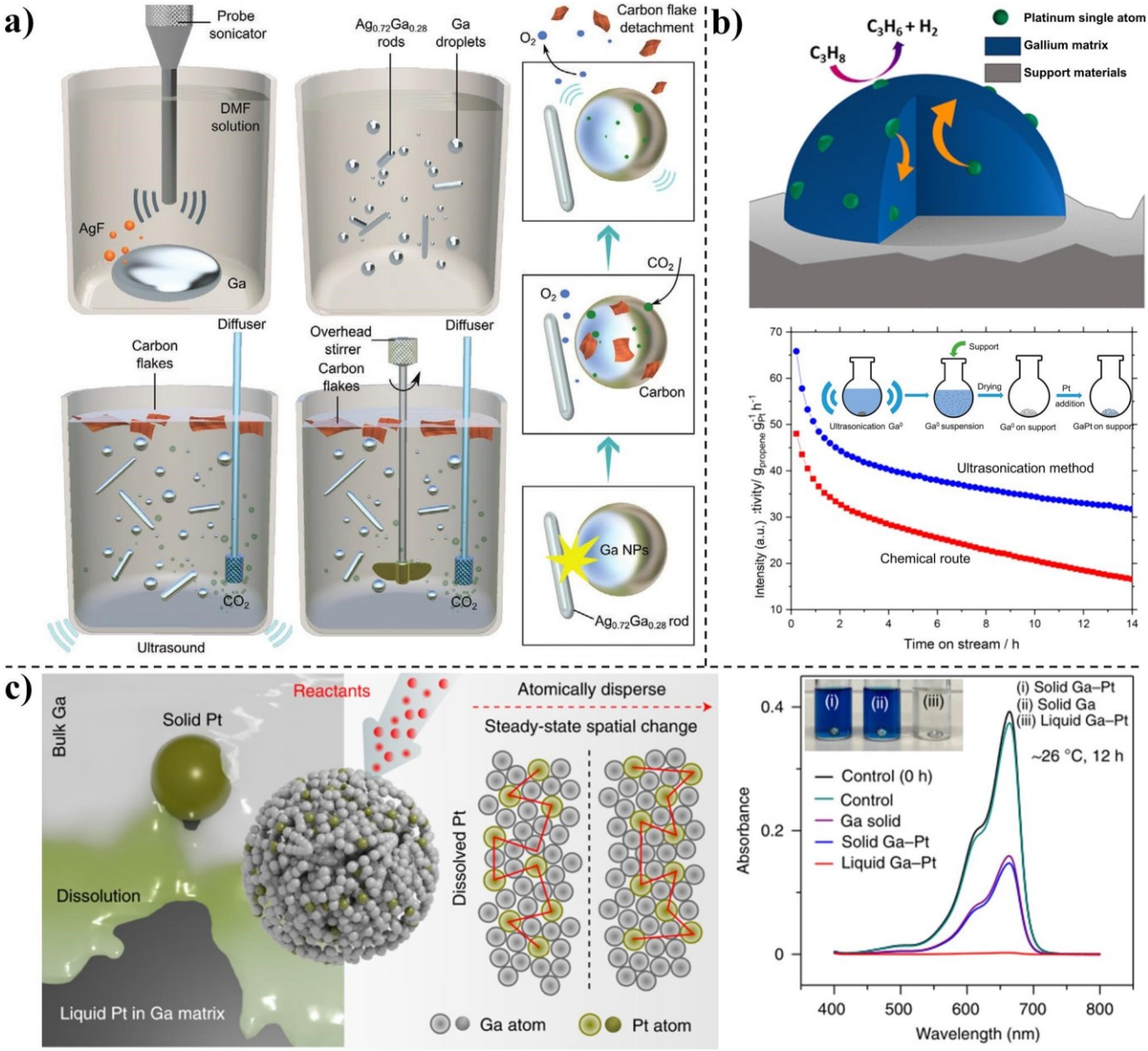

FIGURE 6 Catalysis applications of heterophasic LMs. (a) Mechanism for the production of solid carbon from CO_2 using heterophasic liquid metal. The suspension of catalyst and the CO_2 reduction process can be realized through different mechanical energy inputs. Right: The formation/detachment of the carbon flakes and the generation/escape of O_2 during the CO_2 conversion process. Reproduced with permission.[95] Copyright 2021, Wiley-VCH. (b) Top: Schematic representation of GaPt-SCALMS catalysts for propane dehydrogenation. The Pt atoms moved from the bulk to the surface and back (orange arrows) under high temperature (approximately 300°C). Bottom: Productivity of propane dehydrogenation with different GaPt-SCALMS supported on Al_2O_3 from ultrasonication method (blue symbols) and the chemical route (red symbols). Inset: Schematic illustration for the preparation of GaPt-SCALMS through ultrasonication method. Reproduced with permission.[33] Copyright 2021, American Chemical Society. (c) Left: The preparation and atomic distribution of the Ga-Pt system. The Pt atoms are atomically dispersed and remain dynamic in the Ga matrix due to their natural diffusion. Right: Comparison for the reduction capability of solid and liquid Ga–Pt. Reproduced with permission.[32] Copyright 2022, Springer Nature. LM, liquid metal; SCALMS, supported catalytically active LM solutions.

both Li and Na.[101] Na/Li ions in the Ga-In alloy change the state of LM and heal the surface defects during discharging and charging (Figure 7c). The high theoretical capacity utilization, outstanding cyclic durability, and rate stability make heterophasic LM a promising candidate in the field of energy storage. Owing to the extremely high theoretical energy density and environmental friendliness, lithium-sulfur (Li-S) batteries hold great potential in rechargeable batteries for high-energy storage technologies. A novel dynamic electrocatalytic strategy with solid Sn dynamically distributed in the liquid Ga is proposed to facilitate LiPSs redox reaction[102] (Figure 7d). The EGaSn eutectic alloy effectively improve the performance and cyclic stability of Li-S batteries, expanding the utilization of heterophasic LMs in highspecific-energy batteries. Furthermore, an unprecedented LM battery employing a Na-K alloy anode and Ga-based

28348966, 2023, 1, Downloaded from https://onlinelibrary.wiley.com/doi/10.1002/rpm.20230003, Wiley Online Library on [22/03/2024]. See the Terms and Conditions (https://onlinelibrary.wiley.com/terms-and-conditions) on Wiley Online Library for rules of use; OA articles are governed by the applicable Creative Commons License

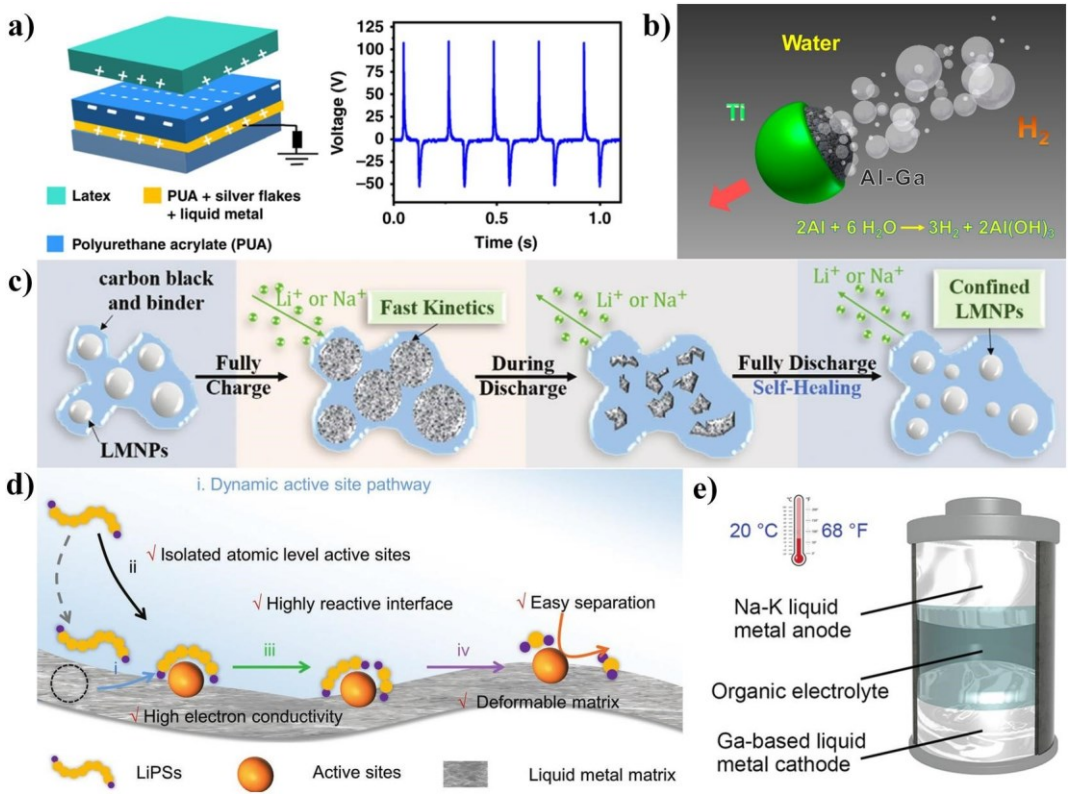

FIGURE 7 Energy applications of heterophasic LMs. (a) Setup and energy-harvesting performance for the SH-TENG. The latex and PUA are used as the positive and negative triboelectric layer, respectively. The polyurethane acrylate, silver flakes, and LM are used as the current collector. The output voltage of the SH-TENG was evaluated when it was subjected to a mechanical force. Reproduced with permission.[99] Copyright 2019, Spring Nature. (b) Schematic image of a water-driven hydrogenpropelled Al-Ga/Ti micromotor. The dark hemisphere (right) and the green area (left) represent the Al-Ga alloy and the asymmetric Ti, respectively. Reproduced with permission.[100] Copyright 2012, American Chemical Society. (c) Schematic images of the anode design and working mechanism for the liquid metal nanoparticle (LMNP) system in a full cell. Reproduced with permission.[101] Copyright 2018, Wiley-VCH. (d) Illustration for the electrochemical performance of dynamic LM electrocatalysts in Li–S batteries. Reproduced with permission.[102] Copyright 2022, Wiley-VCH. (e) Scheme for the room temperature LM battery. Due to the immiscibility and the density difference, the negative electrode (Na-K alloy), electrolyte (organic electrolytes), and positive electrode (Ga-based alloy) self-segregate into three layers. Reproduced with permission.[41] Copyright 2020, Wiley-VCH. LMs, liquid metals; PUA, polyurethane acrylate; SH-TENG, stretchable and healable triboelectric nanogenerator.

alloy cathodes is demonstrated in Figure 7e. Due to immiscibility and the density difference, the negative electrode (Na-K alloy), electrolyte (organic electrolytes), and positive electrode (Ga-based alloy) self-segregate into three layers.[41] Different from the conventional solid electrode and liquid electrolyte, this all-liquid battery delivers stable cycling performance and negligible self-discharge even at −13°C. The self-healing nature, high energy densities, simple battery structures, and high safety of LMs offer them opportunities to build innovative energy-storage devices beyond conventional solid-state batteries.

5 | BIOMEDICAL APPLICATIONS OF HETEROPHASIC LMs

5.1 | Bioimaging and antimicrobial/antiviral properties

Heterophasic LMs have attracted lots of attention in the field of biomaterials owing to the unique photothermal conversion capacity, antimicrobial properties, high electron mobility, fluidity, and excellent biocompatibility.[103,104] Therefore, heterophasic LMs show great potential in the field of antimicrobial and antiviral composites, drug delivery, active treatment of bacterial infection, and broad-spectrum treatment of bacterial biofilms (Table 1).[105,106] Adding metallic elements into LMs can have significant effects on the physical and chemical properties of LM-based composites. Through different approaches, various metals are mixed with LMs, thus forming multi-functional LM-based composites. Doping metallic particles into LMs or producing novel metallic compounds with LMs by chemical reactions is a vital and effective strategy to achieve biomedical applications.[16] In previous research, copper (Cu) has been added into the LMs to achieve biomedical applications such as antimicrobial and antiviral composites, and computed tomography (CT) assistant localization.[42] For example, stretchable electronic skins based on heterophasic LM-Cu show high electrical conductivity and favorable radiological imaging capability (Figure 8a). The electronic skin with Cu particles in LM confirms that metallic compounding is an efficient strategy to

28348966, 2023, 1, Downloaded from https://onlinelibrary.wiley.com/doi/10.1002/rpm.20230003, Wiley Online Library on [22/03/2024]. See the Terms and Conditions (https://onlinelibrary.wiley.com/terms-and-conditions) on Wiley Online Library for rules of use; OA articles are governed by the applicable Creative Commons License

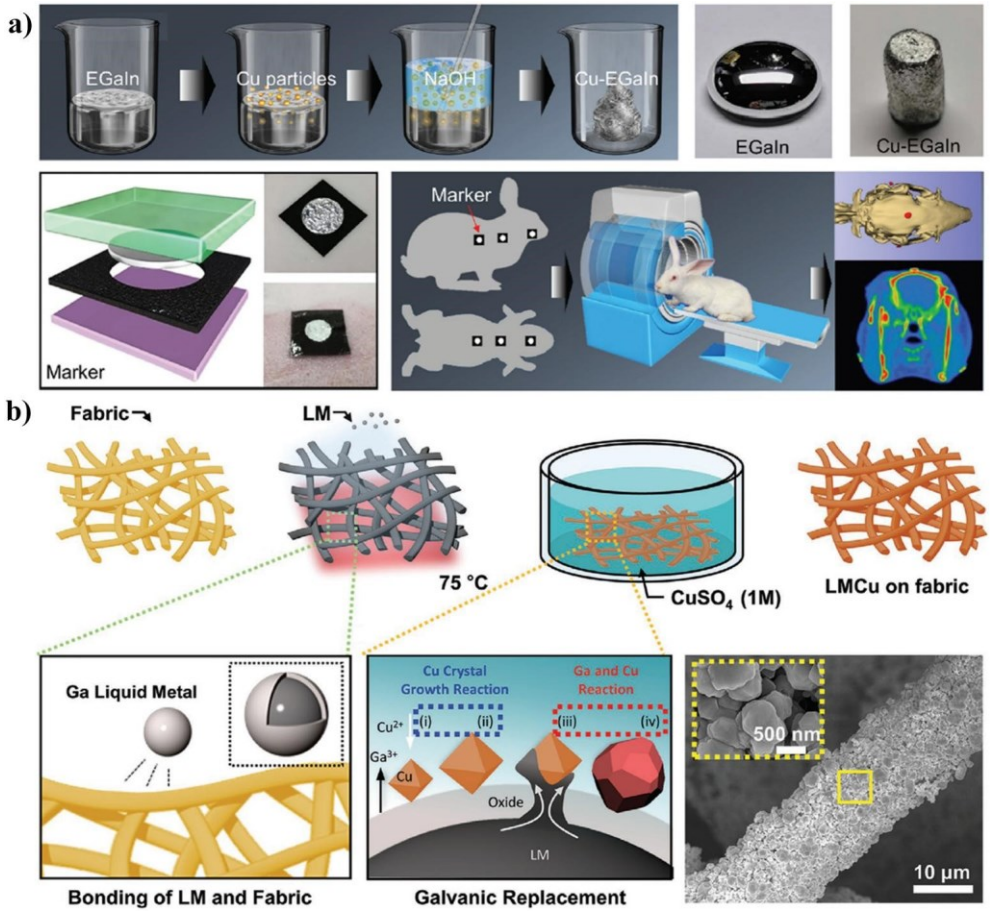

FIGURE 8 Biomedical applications of heterophasic LMs. (a) Top: Preparation of LM-Cu particle composites. Bottom: The structure of the CT assisted localization marker and the effect of the CT assisted localization marker. Reproduced with permission.[42] Copyright 2020, the Royal Society of Chemistry. (b) Top: LM coating scheme on copper fabric. Bottom: Adhesion of LM particles on the fabric by conformal contact and galvanic replacement of LM particles on fabric with Cu ions. SEM images show a single fiber coated with LM-Cu. Adapted with permission.[107] Copyright 2021, Wiley-VCH. CT, computed tomography; LMs, liquid metals.

endow the functionality of CT assisted localization for LMs. Furthermore, Cu particles-based antimicrobial composites have been widely used in daily life and medical fields. A straightforward method has been reported by using LMs to facilitate the deposition of LM-Cu alloys on fabrics to construct antimicrobial and antiviral fabrics[107] (Figure 8b). Compared with pure Cu, LM-Cu alloys have excellent antibacterial, antiviral, and antifungal properties, which enhances the property of copper by mixing it with LMs.

5.2 | Drug delivery and bacterial/tumor treatment

Moreover, heterophasic LM finds proposed use in drug delivery, active treatment of bacterial infection, and broadspectrum treatment of bacterial biofilms.[104,108] Based on the direct doping strategy, heterophasic LM can be applied in bacterial treatment of biomedical fields. For example, researchers have achieved bacterial biofilm physical removement and individual cell rupture by doping LMs into iron (Fe) particles[109] (Figure 9a). The heterophasic LM-Fe exhibits a magneto-responsive characteristic causing spherical particles to undergo shape transformation in a rotating magnetic field. These shape-transformed LM-Fe particle composites exhibit great potential in broad-spectrum applications of antibacterial technology. Besides, by asymmetrical coating LMs on zinc (Zn) particles, researchers can endow Janus structural heterophasic LM-Zn with superb biocompatibility and biodegradability for active target treatment of bacteria[36] (Figure 9b). The motion and self-propulsion of LM-Zn micromotor are achieved by hydrogen bubbles generated from the zinc–acid reaction. Furthermore, the Ga^{III} cations produced from LM-Zn micromotors are served as a built-in antibiotic agent, which enhances antibacterial efficiency against *Helicobacter pylori*. Such LM-Zn micromotors provide an efficient method for the active treatment of bacterial infections. Recently, Pd-based transition metal catalysts have attracted increasing attention in combating diseases. In order to improve the catalytic and therapeutic efficiency of current Pd^0, LM-Pd catalyst has been designed to realize efficient tumor inhibition.[110] The electron-rich

28348966, 2023, 1, Downloaded from https://onlinelibrary.wiley.com/doi/10.1002/rpm.20230003, Wiley Online Library on [22/03/2024]. See the Terms and Conditions (https://onlinelibrary.wiley.com/terms-and-conditions) on Wiley Online Library for rules of use; OA articles are governed by the applicable Creative Commons License

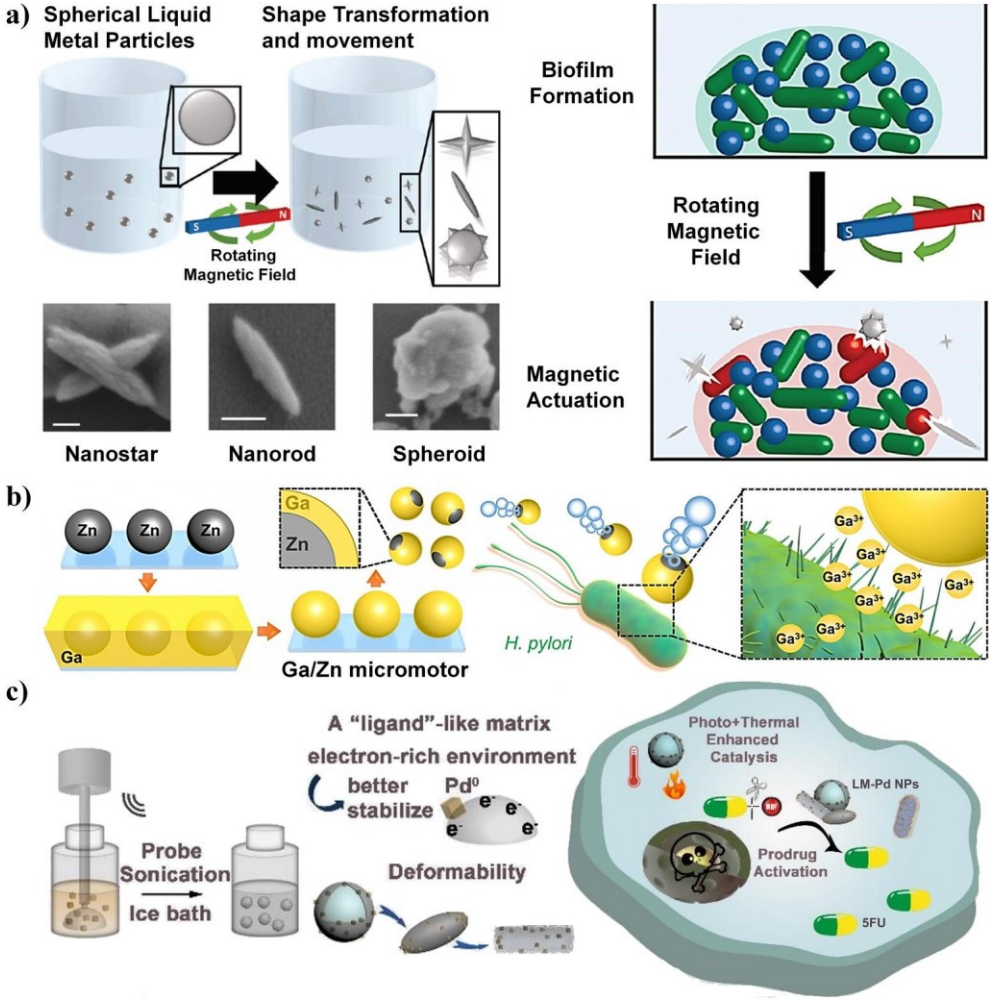

FIGURE 9 Biomedical applications of heterophasic LMs. (a) Left: Schematic demonstration of the shape-transformation of the actuated-LM-Fe particles from spherical to high-aspect-ratio shapes when exposed to a rotating magnetic field; SEM illustration of the range of high-aspect-ratio shapes of actuated-LM-Fe particles, nanostars, nanorods, and spheroids. Right: Scheme for the magneto-physical anti-biofilm activity of the actuated-LM-Fe particles. Reproduced with permission.[109] Copyright 2020, the Royal Society of Chemistry. (b) Left: Scheme for the fabrication of Janus LM-Zn micromotors. Right: The mechanism of the antibacterial activity of LM-Zn micromotors against *Helicobacter pylori* bacteria. Reproduced with permission.[36] Copyright 2021, Wiley-VCH. (c) Left: The fabrication of the LM-Pd NPs. Right: The intracellular prodrug activation for tumor treatment by LM-Pd catalysts. Reproduced with permission.[110] Copyright 2022, Wiley-VCH. LMs, liquid metals.

environment provided by LM ligand can significantly stabilize the active Pd^0 and accelerate the uncaging process of precursor molecules (Figure 9c). Besides, the photothermal effect and photo-enhanced catalysis of LM also contribute to the removal of tumor cells. This work paves the way for the application of heterophasic LM in the biomedical field.

6 | SUMMARY AND OUTLOOK

This review summarizes the research progress of functional heterophasic LMs and their advanced applications in various fields, including sensors, robotics, catalysis, energy management, and biomedical materials (Table 1). Although there are many reports of heterophasic LMs, further investigation is necessary to enable broad applications. Several major challenges and research trends are listed below:

(1) Only a small subset of elements in the periodic table has been introduced into LMs for the functionalization of LMs, therefore exploring new additives may significantly broaden the application of heterophasic LMs. For example, heterophasic LMs with radioactive elements might be used as radioactive tracers for diagnosis or radioactive sources for radiotherapy in the medical field. Besides, introducing alkali metals into different LMs has the promising opportunity to improve the performance of batteries, which is of great importance to the energysaving development in society.

(2) For thousands of years, metals have been widely used as essential materials in all walks of life, while heterophasic LMs are only demonstrated in literature to date. Most of the current research relate to heterophasic LMs flowing at or below room temperature. As a result, their fluidic nature cannot meet the requirement of high moduli needed for structural applications. Interestingly, rigid heterophasic metals can exhibit super-high mechanical robustness through adding new elements such as Bi, In, Zn, and Sn in LMs, which can have special interests for artificial bones and construction materials.

28348966, 2023, 1, Downloaded from https://onlinelibrary.wiley.com/doi/10.1002/rpm.20230003, Wiley Online Library on [22/03/2024]. See the Terms and Conditions (https://onlinelibrary.wiley.com/terms-and-conditions) on Wiley Online Library for rules of use; OA articles are governed by the applicable Creative Commons License

(3) Interfacial issues significantly affect the homogeneity of heterophasic LMs in composite materials, and consequently influence the physical as well as chemical properties of the composites. Polymers and heterophasic LMs readily phase segregate during mixing, increasing the difficulty in forming nano-scaled, uniform and stable materials. Therefore, it is very necessary to explore new strategies to lower the surface energy of heterophasic LMs and disperse nano/micro heterophasic LMs uniformly in the matrix to ensure the high precision/resolution, stability, and durability of the metal-polymer composites for the cutting-edge applications.

(4) Although the phase diagram and fabrication of intermetallic in each phase have been thoroughly investigated, only limited research has focused on the dynamic phase transitions between different metal phases. The properties of heterophasic LMs including morphology, rheology, and electrical/thermal conductivity are tunable through the mediation of the composition and temperature. Besides, phase transitions between metal, metal–nonmental, and binary/TM phase transitions have not been extensively explored. However, versatile phase transitions can improve the performance in applications and enrich functionalities of heterophasic LMs. For example, Fe-C phase diagram occupies a fundamental position in the metallic field, and a small change in carbon content can significantly influence the mechanical properties of the composites. Therefore, phase diagrams could be the key for the investigation and application of heterophasic LMs in the future.

AUTHOR CONTRIBUTIONS

Yan Peng: Investigation; methodology; resources; visualization; writing – original draft; writing – review & editing. **Yumeng Xin**: Resources; writing – original draft. **Jiuyang Zhang**: Conceptualization; formal analysis; funding acquisition; investigation; methodology; project administration; resources; software; supervision; validation; visualization; writing – original draft; writing – review & editing. **Michael D. Dickey**: Conceptualization; formal analysis; methodology; project administration; resources; supervision; validation; visualization; writing – review & editing. **Quan Li**: Conceptualization; formal analysis; investigation; project administration; resources; supervision; validation; writing – original draft; writing – review & editing.

ACKNOWLEDGMENTS

The work is supported by the National Natural Science Foundation of China (Grant No. 52173249, 21774020) and Jiangsu Innovation Team Program.

CONFLICT OF INTEREST STATEMENT

The authors declare no competing interests.

ORCID

Jiuyang Zhang https://orcid.org/0000-0002-9501-5381
Quan Li https://orcid.org/0000-0002-9042-360X

REFERENCES

1. A. Verma, P. Chaudhary, R. K. Tripathi, A. Singh, B. C. Yadav, *J. Inorg. Organomet. Polym. Mater.* **2022**, *32*, 2807.
2. P. M. I. R. Minev, A. Hirsch, Q. Barraud, N. Wenger, E. Martin Moraud, J. Gandar, T. M. Marco Capogrosso, L. Asboth, R. Fajardo Torres, N. Vachicouras, Q. Liu, S. D. P. Natalia, A. Larmagnac, J. Vörös, S. Micera, Z. Suo, G. Courtine, S. P. Lacour, Z. Suo, G. Courtine, *Science* **2015**, *347*, 159.
3. T. Yamada, K. Fukuhara, K. Matsuoka, H. Minemawari, J. Tsutsumi, N. Fukuda, K. Aoshima, S. Arai, Y. Makita, H. Kubo, T. Enomoto, T. Togashi, M. Kurihara, T. Hasegawa, *Nat. Commun.* **2016**, *7*, 11402.
4. C. Xue, Q. Li, *Intelligent Stimuli-Responsive Materials*, Vol. 9 (Ed: Q. Li), John Wiley & Sons, Hoboken, NJ **2013**, p. 293.
5. M. D. Dickey, *Adv. Mater.* **2017**, *29*, 1606425.
6. T. Daeneke, K. Khoshmanesh, N. Mahmood, I. A. de Castro, D. Esrafilzadeh, S. J. Barrow, M. D. Dickey, K. Kalantar-Zadeh, *Chem. Soc. Rev.* **2018**, *47*, 4073.
7. V. Vallem, Y. Sargolzaeiaval, M. Ozturk, Y. C. Lai, M. D. Dickey, *Adv. Mater.* **2021**, *33*, e2004832.
8. M. Woo, *Proc. Natl. Acad. Sci. U. S. A.* **2020**, *117*, 5088.
9. Z. Zhao, S. Soni, T. Lee, C. A. Nijhuis, D. Xiang, *Adv. Mater.* **2022**, *35*, 2203391.
10. S. Chen, R. Zhao, X. Sun, H. Wang, L. Li, J. Liu, *Adv. Healthc. Mater.* **2023**, *12*, e2201924.
11. J. Ma, F. Krisnadi, M. H. Vong, M. Kong, O. M. Awartani, M. D. Dickey, *Adv. Mater.* **2023**, 2205196.
12. Y. Peng, H. Liu, Y. Xin, J. Zhang, *Matter* **2021**, *4*, 3001.
13. S. Wang, X. Zhao, J. Luo, L. Zhuang, D. Zou, *Compos. Part A Appl. Sci. Manuf.* **2022**, *163*, 107216.
14. K. Zuraiqi, A. Zavabeti, F.-M. Allioux, J. Tang, C. K. Nguyen, P. Tafazolymotie, M. Mayyas, A. V. Ramarao, M. Spencer, K. Shah, C. F. McConville, K. Kalantar-Zadeh, K. Chiang, T. Daeneke, *Joule* **2020**, *4*, 2290.
15. X. Sun, H. Li, *RSC Adv.* **2022**, *12*, 24946.
16. N. Yang, F. Gong, J. Ge, L. Wang, G. Wang, L. Cheng, *Mat. Today Nano* **2023**, *21*, 100285.
17. Y. Peng, H. Liu, T. Li, J. Zhang, *ACS Appl. Mater. Interfaces* **2020**, *12*, 6489.
18. Y. Xin, H. Peng, J. Xu, J. Zhang, *Adv. Funct. Mater.* **2019**, *29*, 1808989.
19. B. Chen, M. Wu, S. Fang, Y. Cao, L. Pei, H. Zhong, C. Sun, X. Lin, X. Li, J. Shen, M. Ye, *ACS Nano* **2022**, *16*, 19305.
20. S. Chen, H.-Z. Wang, R.-Q. Zhao, W. Rao, J. Liu, *Matter* **2020**, *2*, 1446.
21. M. Tavakoli, P. Alhais Lopes, A. Hajalilou, A. F. Silva, M. Reis Carneiro, J. Carvalheiro, J. Marques Pereira, A. T. de Almeida, *Adv. Mater.* **2022**, *34*, e2203266.
22. W. Xing, H. Wang, S. Chen, P. Tao, W. Shang, B. Fu, C. Song, T. Deng, *Adv. Eng. Mater.* **2022**, *24*, 2101678.
23. Y. Zhang, S. Jiang, Y. Hu, T. Wu, Y. Zhang, H. Li, A. Li, Y. Zhang, H. Wu, Y. Ding, E. Li, J. Li, D. Wu, Y. Song, J. Chu, *Nano Lett.* **2022**, *22*, 2923.
24. Y. Lu, Y. Lin, Z. Chen, Q. Hu, Y. Liu, S. Yu, W. Gao, M. D. Dickey, Z. Gu, *Nano Lett.* **2017**, *17*, 2138.
25. X. Wang, L. Fan, J. Zhang, X. Sun, H. Chang, B. Yuan, R. Guo, M. Duan, J. Liu, *Adv. Funct. Mater.* **2019**, *29*, 1907063.
26. M. H. Malakooti, M. R. Bockstaller, K. Matyjaszewski, C. Majidi, *Nanoscale Adv.* **2020**, *2*, 2668.
27. Y. Liu, W. Zhang, H. Wang, *Mater. Horiz.* **2021**, *8*, 56.
28. F. Carle, K. Bai, J. Casara, K. Vanderlick, E. Brown, *Phys. Rev. Fluids* **2017**, *2*, 013301.
29. M. Sun, C. Tian, L. Mao, X. Meng, X. Shen, B. Hao, X. Wang, H. Xie, L. Zhang, *Adv. Funct. Mater.* **2022**, *32*, 2112508.
30. M. Liu, Y. Wang, Y. Kuai, J. Cong, Y. Xu, H. G. Piao, L. Pan, Y. Liu, *Small* **2019**, *15*, e1905446.
31. R. Guo, X. Sun, B. Yuan, H. Wang, J. Liu, *Adv. Sci.* **2019**, *6*, 1901478.
32. M. A. Rahim, J. Tang, A. J. Christofferson, P. V. Kumar, N. Meftahi, F. Centurion, Z. Cao, J. Tang, M. Baharfar, M. Mayyas, F. M. Allioux, P. Koshy, T. Daeneke, C. F. McConville, R. B. Kaner, S. P. Russo, K. Kalantar-Zadeh, *Nat. Chem.* **2022**, *14*, 935.

28348966, 2023, 1, Downloaded from https://onlinelibrary.wiley.com/doi/10.1002/rpm.20230003, Wiley Online Library on [22/03/2024]. See the Terms and Conditions (https://onlinelibrary.wiley.com/terms-and-conditions) on Wiley Online Library for rules of use; OA articles are governed by the applicable Creative Commons License

33. N. Raman, M. Wolf, M. Heller, N. Heene-Wurl, N. Taccardi, M. Haumann, P. Felfer, P. Wasserscheid, *ACS Catal.* **2021**, *11*, 13423.
34. N. Raman, S. Maisel, M. Grabau, N. Taccardi, J. Debuschewitz, M. Wolf, H. Wittkamper, T. Bauer, M. Wu, M. Haumann, C. Papp, A. Gorling, E. Spiecker, J. Libuda, H. P. Steinruck, P. Wasserscheid, *ACS Catal.* **2019**, *9*, 9499.
35. V. Feig, E. Remlova, B. Muller, J. L. P. Kuosmanen, N. Lal, A. Ginzburg, K. Nan, A. Patel, A. M. Jebran, M. P. Bantwal, N. Fabian, K. Ishida, J. Jenkins, J. G. Rosenboom, S. Park, W. Madani, A. Hayward, G. Traverso, *Adv. Mater.* **2023**, *35*, 2208227.
36. Z. Lin, C. Gao, D. Wang, Q. He, *Angew. Chem. Int. Ed.* **2021**, *60*, 8750.
37. P. A. Lopes, B. C. Santos, A. T. de Almeida, M. Tavakoli, *Nat. Commun.* **2021**, *12*, 4666.
38. H. Wang, Y. Peng, H. Peng, J. Zhang, *Proc. Natl. Acad. Sci. U. S. A.* **2022**, *119*, e2200223119.
39. I. A. Castor, A. F. Chrimes, A. Zavabeti, K. J. Berean, B. J. Carey, J. Zhuang, Y. Du, S. X. Dou, K. Suzuki, R. A. Shanks, R. Nixon-Luke, G. Bryant, K. Khoshmanesh, K. Kalantar-Zadeh, T. Daeneke, *Nano Lett.* **2017**, *17*, 7831.
40. H. Wang, S. Chen, H. Li, X. Chen, J. Cheng, Y. Shao, C. Zhang, J. Zhang, L. Fan, H. Chang, R. Guo, X. Wang, N. Li, L. Hu, Y. Wei, J. Liu, *Adv. Funct. Mater.* **2021**, *31*, 2100274.
41. Y. Ding, X. Guo, Y. Qian, L. Xue, A. Dolocan, G. Yu, *Adv. Mater.* **2020**, *32*, e2002577.
42. R. Guo, B. Cui, X. Zhao, M. Duan, X. Sun, R. Zhao, L. Sheng, J. Liu, J. Lu, *Mater. Horiz.* **2020**, *7*, 1845.
43. X. Guo, L. Zhang, Y. Ding, J. B. Goodenough, G. Yu, *Energy Environ. Sci.* **2019**, *12*, 2605.
44. H. Bark, P. S. Lee, *Chem. Sci.* **2021**, *12*, 2760.
45. H. Liu, Y. Xin, H. K. Bisoyi, Y. Peng, J. Zhang, Q. Li, *Adv. Mater.* **2021**, *33*, e2104634.
46. L. Ren, X. Xu, Y. Du, K. Kalantar-Zadeh, S. X. Dou, *Mater. Today* **2020**, *34*, 92.
47. S. Liu, D. S. Shah, R. Kramer-Bottiglio, *Nat. Mater.* **2021**, *20*, 851.
48. F. Li, S. Gao, Y. Lu, W. Asghar, J. Cao, C. Hu, H. Yang, Y. Wu, S. Li, J. Shang, M. Liao, Y. Liu, R. W. Li, *Adv. Sci.* **2021**, *8*, 2004208.
49. Y. Wu, Z. Deng, Z. Peng, R. Zheng, S. Liu, S. Xing, J. Li, D. Huang, L. Liu, *Adv. Funct. Mater.* **2019**, *29*, 1903840.
50. M. Tavakoli, M. H. Malakooti, H. Paisana, Y. Ohm, D. G. Marques, P. Alhais Lopes, A. P. Piedade, A. T. de Almeida, C. Majidi, *Adv. Mater.* **2018**, *30*, e1801852.
51. J. Wang, G. Cai, S. Li, D. Gao, J. Xiong, P. S. Lee, *Adv. Mater.* **2018**, *30*, e1706157.
52. B. J. Blaiszik, S. L. Kramer, M. E. Grady, D. A. McIlroy, J. S. Moore, N. R. Sottos, S. R. White, *Adv. Mater.* **2012**, *24*, 398.
53. B. Deng, G. J. Cheng, *Adv. Mater.* **2019**, *31*, e1807811.
54. D. Xu, J. Cao, F. Liu, S. Zou, W. Lei, Y. Wu, Y. Liu, J. Shang, R. W. Li, *Sensors* **2022**, *22*, 2516.
55. Y. Ding, X. Guo, G. Yu, *ACS Cent. Sci.* **2020**, *6*, 1355.
56. P. Lv, X. Yang, H. K. Bisoyi, H. Zeng, X. Zhang, Y. Chen, P. Xue, S. Shi, A. Priimagi, L. Wang, W. Feng, Q. Li, *Mater. Horiz.* **2021**, *8*, 2475.
57. S. A. Idrus-Saidi, J. Tang, S. Lambie, J. Han, M. Mayyas, M. B. Ghasemian, F.-M. Allioux, S. Cai, P. Koshy, P. Mostaghimi, K. G. Steenbergen, A. S. Barnard, T. Daeneke, N. Gaston, K. KalantarZadeh, *Science* **2022**, *378*, 1118.
58. M. Mayyas, M. Mousavi, M. B. Ghasemian, R. Abbasi, H. Li, M. J. Christoe, J. Han, Y. Wang, C. Zhang, M. A. Rahim, J. Tang, J. Yang, D. Esrafilzadeh, R. Jalili, F. M. Allioux, A. P. O'Mullane, K. Kalantar-Zadeh, *ACS Nano* **2020**, *14*, 14070.
59. W. Kong, Z. Wang, M. Wang, K. C. Manning, A. Uppal, M. D. Green, R. Y. Wang, K. Rykaczewski, *Adv. Mater.* **2019**, *31*, e1904309.
60. L. Ren, S. Sun, G. Casillas-Garcia, M. Nancarrow, G. Peleckis, M. Turdy, K. Du, X. Xu, W. Li, L. Jiang, S. X. Dou, Y. Du, *Adv. Mater.* **2018**, *30*, 1802595.
61. R. David, N. Miki, *Nanoscale* **2019**, *11*, 21419.
62. S. Bhagwat, C. O'Brien, A. Hamza, S. Sharma, C. Rein, M. Sanjaya, D. Helmer, F. Kotz-Helmer, P. Pezeshkpour, B. E. Rapp, *Adv. Mater.* **2022**, *34*, e2201469.
63. J. Shu, D. A. Ge, E. Wang, H. Ren, T. Cole, S. Y. Tang, X. Li, X. Zhou, R. Li, H. Jin, W. Li, M. D. Dickey, S. Zhang, *Adv. Mater.* **2021**, *33*, e2103062.
64. E. J. Markvicka, M. D. Bartlett, X. Huang, C. Majidi, *Nat. Mater.* **2018**, *17*, 618.
65. Y. Xin, J. Lan, J. Xu, D. Wu, J. Zhang, *ACS Appl. Mater. Interfaces* **2021**, *13*, 19351.
66. A. Hajalilou, A. F. Silva, P. A. Lopes, E. Parvini, C. Majidi, M. Tavakoli, *Adv. Mater. Interfaces* **2022**, *9*, 2101913.
67. G. Yun, S.-Y. Tang, Q. Zhao, Y. Zhang, H. Lu, D. Yuan, S. Sun, L. Deng, M. D. Dickey, W. Li, *Matter* **2020**, *3*, 824.
68. G. Yun, S.-Y. Tang, S. Sun, D. Yuan, Q. Zhao, L. Deng, S. Yan, H. Du, M. D. Dickey, W. Li, *Nat. Commun.* **2019**, *10*, 1300.
69. Y. Wang, W. Duan, C. Zhou, Q. Liu, J. Gu, H. Ye, M. Li, W. Wang, X. Ma, *Adv. Mater.* **2019**, *31*, e1905067.
70. A. Hirsch, H. O. Michaud, A. P. Gerratt, S. de Mulatier, S. P. Lacour, *Adv. Mater.* **2016**, *28*, 4507.
71. M. Reis Carneiro, C. Majidi, M. Tavakoli, *Adv. Funct. Mater.* **2022**, *32*, 2205956.
72. G. H. Lee, H. Woo, C. Yoon, C. Yang, J. Y. Bae, W. Kim, D. H. Lee, H. Kang, S. Han, S. K. Kang, S. Park, H. R. Kim, J. W. Jeong, S. Park, *Adv. Mater.* **2022**, *34*, e2204159.
73. C. Cho, W. Shin, M. Kim, J. Bang, P. Won, S. Hong, S. H. Ko, *Small* **2022**, *18*, e2202841.
74. R. Zheng, Z. Peng, Y. Fu, Z. Deng, S. Liu, S. Xing, Y. Wu, J. Li, L. Liu, *Adv. Funct. Mater.* **2020**, *30*, 1910524.
75. H. Peng, W. Luo, Y. Peng, Y. Chen, J. Zhang, W. Hu, *Sci. China Mater.* **2022**, *66*, 1124.
76. B. Ma, C. Xu, J. Chi, J. Chen, C. Zhao, H. Liu, *Adv. Funct. Mater.* **2019**, *29*, 1901370.
77. H. Wang, W. Xing, S. Chen, C. Song, M. D. Dickey, T. Deng, *Adv. Mater.* **2021**, *33*, e2103104.
78. M. I. Ralphs, N. Kemme, P. B. Vartak, E. Joseph, S. Tipnis, S. Turnage, K. N. Solanki, R. Y. Wang, K. Rykaczewski, *ACS Appl. Mater. Interfaces* **2018**, *10*, 2083.
79. J. Tang, X. Zhao, J. Li, R. Guo, Y. Zhou, J. Liu, *ACS Appl. Mater. Interfaces* **2017**, *9*, 35977.
80. D. P. Parekh, C. M. Fancher, M. G. Mohammed, T. V. Neumann, D. Saini, J. Guerrier, C. Ladd, E. Hubbard, J. L. Jones, M. D. Dickey, *ACS Appl. Nano Mater.* **2020**, *3*, 12064.
81. R. Tutika, S. H. Zhou, R. E. Napolitano, M. D. Bartlett, *Adv. Funct. Mater.* **2018**, *28*, 1804336.
82. G. A. P. Yoonho Kim, S. Liu, X. Zhao, *Sci. Robot.* **2019**, *4*, eaax7329.
83. H. Zhou, C. C. Mayorga-Martinez, S. Pane, L. Zhang, M. Pumera, *Chem. Rev.* **2021**, *121*, 4999.
84. M. Wang, T. Hu, H. K. Bisoyi, Z. Yu, L. Liu, Y. Song, J. Yang, H. Yang, Q. Li, *Small* **2022**, *19*, e2204609.
85. L. Cao, D. Yu, Z. Xia, H. Wan, C. Liu, T. Yin, Z. He, *Adv. Mater.* **2020**, *32*, e2000827.
86. Q. Wang, C. Pan, Y. Zhang, L. Peng, Z. Chen, C. Majidi, L. Jiang, *Matter* **2023**, *6*, 855.
87. H. Kim, K. Lee, J. W. Oh, Y. Kim, J. E. Park, J. Jang, S. W. Lee, S. Lee, C. M. Koo, C. Park, *Adv. Funct. Mater.* **2022**, *33*, 2210385.
88. J. Zhang, R. H. Soon, Z. Wei, W. Hu, M. Sitti, *Adv. Sci.* **2022**, *9*, e2203730.
89. H. Liu, J. Xia, N. Zhang, H. Cheng, W. Bi, X. Zu, W. Chu, H. Wu, C. Wu, Y. Xie, *Nat. Catal.* **2021**, *4*, 202.
90. E. A. Redekop, V. V. Galvita, H. Poelman, V. Bliznuk, C. Detavernier, G. B. Marin, *ACS Catal.* **2014**, *4*, 1812.
91. N. Taccardi, M. Grabau, J. Debuschewitz, M. Distaso, M. Brandl, R. Hock, F. Maier, C. Papp, J. Erhard, C. Neiss, W. Peukert, A. Gorling, H. P. Steinruck, P. Wasserscheid, *Nat. Chem.* **2017**, *9*, 862.
92. I. Sharafutdinov, C. F. Elkjær, H. W. Pereira de Carvalho, D. Gardini, G. L. Chiarello, C. D. Damsgaard, J. B. Wagner, J.-D. Grunwaldt, S. Dahl, I. Chorkendorff, *J. Catal.* **2014**, *320*, 77.

28348966, 2023, 1, Downloaded from https://onlinelibrary.wiley.com/doi/10.1002/rpm.20230003, Wiley Online Library on [22/03/2024]. See the Terms and Conditions (https://onlinelibrary.wiley.com/terms-and-conditions) on Wiley Online Library for rules of use; OA articles are governed by the applicable Creative Commons License

93. F. Studt, I. Sharafutdinov, F. Abild-Pedersen, C. F. Elkjaer, J. S. Hummelshoj, S. Dahl, I. Chorkendorff, J. K. Norskov, *Nat. Chem.* **2014**, *6*, 320.
94. F. Hoshyargar, J. Crawford, A. P. O'Mullane, *J. Am. Chem. Soc.* **2017**, *139*, 1464.
95. J. Tang, M. Mayyas, M. B. Ghasemian, J. Sun, M. A. Rahim, J. Yang, J. Han, D. J. Lawes, R. Jalili, T. Daeneke, M. G. Saborio, Z. Cao, C. A. Echeverria, F. M. Allioux, A. Zavabeti, J. Hamilton, V. Mitchell, A. P. O'Mullane, R. B. Kaner, D. Esrafilzadeh, M. D. Dickey, K. Kalantar-Zadeh, *Adv. Mater.* **2022**, *34*, e2105789.
96. S. Lambie, K. G. Steenbergen, N. Gaston, *Angew. Chem. Int. Ed.* **2023**, *62*, e202219009.
97. X. Wang, W. Yao, R. Guo, X. Yang, J. Tang, J. Zhang, W. Gao, V. Timchenko, J. Liu, *Adv. Healthc. Mater.* **2018**, *7*, e1800318.
98. S. N. S. Hapuarachchi, K. C. Wasalathilake, D. P. Siriwardena, J. Y. Nerkar, H. Chen, S. Zhang, Y. Liu, J. Zheng, D. V. Golberg, A. P. O'Mullane, C. Yan, *ACS Appl. Energy Mater.* **2020**, *3*, 5147.
99. K. Parida, G. Thangavel, G. Cai, X. Zhou, S. Park, J. Xiong, P. S. Lee, *Nat. Commun.* **2019**, *10*, 2158.
100. Wei Gao, A. Pei, J. Wang, *ACS Nano* **2012**, *6*, 8432.
101. X. Guo, Y. Ding, L. Xue, L. Zhang, C. Zhang, J. B. Goodenough, G. Yu, *Adv. Funct. Mater.* **2018**, *28*, 1804649.
102. Y. Qi, N. Li, K. Zhang, Y. Yang, Z. Ren, J. You, Q. Hou, C. Shen, T. Jin, Z. Peng, K. Xie, *Adv. Mater.* **2022**, *34*, e2204810.
103. L. Yi, J. Liu, *Int. Mater. Rev.* **2017**, *62*, 415.
104. J. Yan, Y. Lu, G. Chen, M. Yang, Z. Gu, *Chem. Soc. Rev.* **2018**, *47*, 2518.
105. X. Sun, B. Yuan, L. Sheng, W. Rao, J. Liu, *Appl. Mater. Today* **2020**, *20*, 100722.
106. W. Gao, Y. Wang, Q. Wang, G. Ma, J. Liu, *J. Mater. Chem. B* **2022**, *10*, 829.
107. K. Y. Kwon, S. Cheeseman, A. Frias-De-Diego, H. Hong, J. Yang, W. Jung, H. Yin, B. J. Murdoch, F. Scholle, N. Crook, E. Crisci, M. D. Dickey, V. K. Truong, T. I. Kim, *Adv. Mater.* **2021**, *33*, e2104298.
108. L. Wang, R. Lai, L. Zhang, M. Zeng, L. Fu, *Adv. Mater.* **2022**, *34*, e2201956.
109. S. Cheeseman, A. Elbourne, R. Kariuki, A. V. Ramarao, A. Zavabeti, N. Syed, A. J. Christofferson, K. Y. Kwon, W. Jung, M. D. Dickey, K. Kalantar-Zadeh, C. F. McConville, R. J. Crawford, T. Daeneke, J. Chapman, V. K. Truong, *J. Mater. Chem. B* **2020**, *8*, 10776.
110. L. Zhang, Y. Sang, Z. Liu, W. Wang, Z. Liu, Q. Deng, Y. You, J. Ren, X. Qu, *Angew. Chem. Int. Ed.* **2022**, *62*, e202218159.

AUTHOR BIOGRAPHIES

Yan Peng is currently a Ph.D. student in the School of Chemistry and Chemical Engineering, Southeast University. Her research mainly focuses on metal-polymer composites for responsive materials, flexible electronics, and self-healing materials.

Yumeng Xin received his Ph.D. degree in Materials Physics and Chemistry from the School of Chemistry and Chemical Engineering at Southeast University in 2021. He is currently a lecturer in the School of Environmental and Chemical Engineering at Jiangsu Ocean University. His research focuses on metal-polymer composites for wearable electronic devices.

Jiuyang Zhang obtained his PhD from University of South Carolina, Columbia, in the Department of Chemistry and Biochemistry in 2014. He is currently a Professor at the School of Chemistry and Chemical Engineering, Southeast University. His research interests are metal-polymer composites and polymer electronic materials.

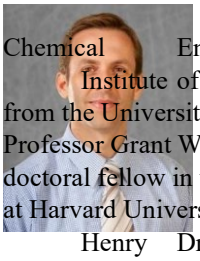

Michael D. Dickey received a BS in Chemical Engineering from the Georgia Institute of Technology (1999) and a PhD from the University of Texas (2006) under the guidance of Professor Grant Willson. From 2006– 2008 he was a post-doctoral fellow in the lab of Professor George Whitesides at Harvard University. He is currently the Camille and Henry Dreyfus Professor in the Department of Chemical and Biomolecular Engineering at NC State University. He completed a sabbatical at Microsoft in 2016. Michael's research interests include soft matter (liquid metals, gels, and polymers) for soft and stretchable devices (electronics, energy harvesters, textiles, and soft robotics).

28348966, 2023, 1, Downloaded from https://onlinelibrary.wiley.com/doi/10.1002/rpm.20230003, Wiley Online Library on [22/03/2024]. See the Terms and Conditions (https://onlinelibrary.wiley.com/terms-and-conditions) on Wiley Online Library for rules of use; OA articles are governed by the applicable Creative Commons License

Quan Li is Distinguished Chair Professor and universities. His current research interest spans from stimuli-responsive smart soft matter, advanced photonics, and optoelectronic materials for energy harvesting and energy saving to functional biocompatible materials and nanoparticles to nanoengineering and device fabrication.

How to cite this article: Y. Peng, Y. Xin, J. Zhang, M. D. Dickey, Q. Li, *Responsive Mater.* **2023**, *1*, e20230003. https://doi.org/10.1002/rpm.20230003

28348966, 2023, 1, Downloaded from https://onlinelibrary.wiley.com/doi/10.1002/rpm.20230003, Wiley Online Library on [22/03/2024]. See the Terms and Conditions (https://onlinelibrary.wiley.com/terms-and-conditions) on Wiley Online Library for rules of use; OA articles are governed by the applicable Creative Commons L

Director of Institute of Advanced Materials at Southeast University. He held appointments in USA, Germany, and France. Li received his Ph.D. from the Chinese Academy of Sciences in Shanghai, where he was promoted to a youngest Full Professor in February 1998. He is a Fellow of the Royal Society of Chemistry. He has been elected as a member of the European Academy of Sciences and the European Academy of Sciences and Arts. He has also been honored as Professor and Chair Professor at several